Seasonal and diurnal variations of methane and carbon dioxide in the Kathmandu Valley in the foothills of the central Himalaya

Khadak Singh Mahata[1,2], Arnico Kumar Panday [3,4], Maheswar Rupakheti[1,5*], Ashish Singh[1], Manish Naja[6], Mark G. Lawrence[1,2]

[1] Institute for Advanced Sustainability Studies (IASS), Potsdam, Germany

[2] University of Potsdam, Potsdam, Germany

[3] International Centre for Integrated Mountain Development (ICIMOD), Lalitpur, Nepal

[4] University of Virginia, Virginia, USA

[5] Himalayan Sustainability Institute (HIMSI), Kathmandu, Nepal

[6] Aryabhatta Research Institute of Observational Sciences (ARIES), Nainital, India

*Correspondence to: M. Rupakheti (maheswar.rupakheti@iass-potsdam.de)

Abstract

The SusKat-ABC (Sustainable Atmosphere for the Kathmandu Valley- Atmospheric Brown Clouds) international air pollution measurement campaign was carried out during December 2012-June 2013 in the Kathmandu Valley and surrounding regions in Nepal. The Kathmandu Valley is a bowl-shaped basin with a severe air pollution problem. This paper reports measurements of two major greenhouse gases (GHGs), methane (CH_4) and carbon dioxide (CO_2), along with the pollutant CO, that began during the campaign and were extended for a year at the SusKat-ABC supersite in Bode, a semi-urban location in the Kathmandu Valley. Simultaneous measurements were also made during 2015 in Bode and a nearby rural site (Chanban), ~25 km (aerial distance) to the southwest of Bode, on the other side of a tall ridge. The ambient mixing ratios of methane (CH_4), carbon dioxide (CO_2), water vapor, and carbon monoxide (CO) were measured with a cavity ring down spectrometer (Picarro G2401, USA),

along with meteorological parameters for a year (March 2013 - March 2014). These measurements are the first of their kind in the central Himalayan foothills. At Bode, the annual average mixing ratios of CO_2 and CH_4 were 419.3 (±6.0) ppm and 2.192 (±0.066) ppm, respectively. These values are higher than the levels observed at background sites such as Mauna Loa, USA (CO_2: 396.8 ± 2.0 ppm, CH_4: 1.831 ± 0.110 ppm) and Waliguan, China (CO_2: 397.7 ± 3.6 ppm, CH_4: 1.879 ± 0.009 ppm) during the same period, and at other urban and semi-urban sites in the region such as Ahmedabad and Shadnagar (India). They varied slightly across the seasons at Bode, with seasonal average CH_4 mixing ratios being 2.157 (±0.230) ppm in the pre-monsoon season, 2.199 (±0.241) ppm in the monsoon, 2.210 (±0.200) ppm in the post-monsoon, and 2.214 (± 0.209) ppm in the winter season. The average CO_2 mixing ratios were 426.2 (±25.5) ppm in pre-monsoon, 413.5 (±24.2) ppm in monsoon, 417.3 (±23.1) ppm in post-monsoon, and 421.9 (±20.3) ppm in winter season. The maximum seasonal mean mixing ratio of CH_4 in winter was only 0.057 ppm or 2.6 % higher than the seasonal minimum during the pre-monsoon period, while CO_2 was 12.8 ppm or 3.1 % higher during the pre-monsoon period (seasonal maximum) than during the monsoon (seasonal minimum). On the other hand, the CO mixing ratio at Bode was 191 % higher during the winter than during the monsoon season. The enhancement in CO_2 mixing ratios during the pre-monsoon season is associated with additional CO_2 emissions from forest fire and agro-residue burning in northern South Asia in addition to local emissions in the Kathmandu Valley. Published CO/CO_2 ratios of different emission sources in Nepal and India were compared with the observed CO/CO_2 ratios in this study. This comparison suggested that the major sources in the Kathmandu Valley were residential cooking and vehicle exhaust in all seasons except winter. In winter, the brick kiln emissions were a major source. Simultaneous measurement in Bode and Chanban (15 July - 3 Oct 2015) revealed that the mixing ratio of CO_2, CH_4 and CO mixing ratios were 3.8 %, 12 %, and 64 % higher in Bode than Chanban. Kathmandu Valley, thus, has significant emissions from local sources, which can also be attributed to its bowl shaped geography that is conducive to pollution build-up. At Bode, all three gas species (CO_2, CH_4 and CO) showed strong diurnal patterns in their mixing ratios with a pronounced morning peak (ca. 08:00), a dip in the afternoon, and again gradual increase through the night until the next morning, whereas CH_4 and CO at Chanban did not show any noticeable diurnal variations.

These measurements provide the first insights into diurnal and seasonal variation of key greenhouse gases and air pollutants and their local and regional sources, which are important information for the atmospheric research in the region.

1 Introduction

The average atmospheric mixing ratios of two major greenhouse gases (GHGs), CO_2 and CH_4, have increased by about 40 % (from 278 to 390.5 ppm) and about 150 % (from 722 to 1803 ppb) respectively since pre-industrial times (~1750 AD). This is mostly attributed to anthropogenic emissions (IPCC, 2013). The current global annual rate of increase of the atmospheric CO_2 mixing ratio is 1-3 ppm, with average annual mixing ratios now exceeding a value of 400 ppm at the background reference location in Mauna Loa (WMO, 2016). Between 1750 and 2011, 240(±10) Pg C of anthropogenic CO_2 was accumulated in the atmosphere of which two thirds were contributed by fossil fuel combustion and cement production, with the remaining coming from deforestation and land use/land cover changes (IPCC, 2013). CH_4 is the second largest gaseous contributor to anthropogenic radiative forcing after CO_2 (Forster et al., 2007). The major anthropogenic sources of atmospheric CH_4 are rice paddies, ruminants and fossil fuel use, contributing approximately 60 % to the global CH_4 budget (Chen and Prinn, 2006; Schneising et al., 2009). The remaining fraction is contributed by biogenic sources such as wetlands and fermentation of organic matter by microbes in anaerobic conditions (Conrad, 1996).

Increasing atmospheric mixing ratios of CO_2 and CH_4 and other GHGs and short-lived climate-forcing pollutants (SLCPs) such as black carbon (BC) and tropospheric ozone (O_3) have caused the global mean surface temperature to increase by 0.85 °C from 1880 to 2012. The surface temperature is expected to increase further by up to 2 degrees at the end of the 21st century in most representative concentration pathways (RCPs) emission scenarios (IPCC, 2013). The increase in surface temperature is linked to melting of glaciers and ice sheets, sea level rise, extreme weather events, loss of biodiversity, reduced crop productivity, and economic losses (Fowler and Hennessy, 1995; Guoxin and Shibasaki, 2003).

Seventy percent of global anthropogenic CO_2 is emitted in urban areas (Fragkias et al., 2013). Developing countries may have lower per capita GHG emissions than developed countries, but the large cities in developing countries, with their high population and industrial densities, are major consumers of fossil fuels and thus, emitters of GHGs. South Asia, a highly populated region with rapid growth in urbanization, motorization, and industrialization in recent decades, has an ever increasing fossil fuel demand and its combustion emitted 444 Tg C yr^{-1} in 2000 (Patra, et al., 2013), or about 5 % of the global total CO_2 emissions. Furthermore, a major segment of the population in South Asia has an agrarian economy and uses biofuel for cooking activities, and agro-residue burning is also common practice in the region, which are important major sources of air pollutants and greenhouse gases in the region (CBS, 2011; Pandey et al., 2014; Sinha et al., 2014).

The emission and uptake of CO_2 and CH_4 follow a distinct cycle in South Asia. By using inverse modeling, Patra et al. (2011) found a net CO_2 uptake (0.37 ± 0.20 Pg C yr^{-1}) during 2008 in South Asia and the uptake (sink) is highest during July-September. The remaining months act~~s~~ as a weak gross sink but a moderate gross source for CO_2 in the region. The observed variation is linked with the growing seasons. Agriculture is a major contributor of methane emission. For instance, in India it contributes to 75 % of CH_4 emissions (MoEF, 2007). Ambient CH_4 concentrations are highest during June to September (peaking in September) in South Asia which are also the growing months for rice paddies (Goroshi et al., 2011). The minimum column averaged CH_4 mixing ratios are in February-March (Prasad et al., 2014).

Climate change has impacted South Asia in several ways, as evident in temperature increase, change in precipitation patterns, higher incidence of extreme weather events (floods, droughts, heat waves, cold waves), melting of snowfields and glaciers in the mountain regions, and impacts on ecosystems and livelihoods (ICIMOD, 2009; MoE, 2011). Countries such as Nepal are vulnerable to impacts of climate change due to inadequate preparedness for adaptation to impacts of climate change (MoE, 2011). Decarbonization of its economy can be an important policy measure in mitigating climate change. Kathmandu Valley is one of the largest metropolitan cities in the foothills of the Hindu Kush-Himalaya which has significant reliance on fossil fuels and biofuels. In 2005, fossil fuel burning accounted for 53 % of total energy

consumption in the Kathmandu Valley, while biomass and hydroelectricity were 38 % and 9 %, respectively (Shrestha and Rajbhandari, 2010). Fossil fuel consumed in the Kathmandu Valley accounts for 32 % of the country's fossil fuel imports, and the major fossil fuel consumers are residential (53.17 %), transport (20.80 %), industrial (16.84 %), and commercial (9.11 %) sectors. Combustion of these fuels in traditional technologies such as Fixed Chimney Bulls Trench Kiln (FCBTK) and low efficiency engines (vehicles, captive power generator sets etc.) emit significant amounts of greenhouse gases and air pollutants. This has contributed to elevated ambient concentrations of particulate matter (PM), including black carbon and organic carbon, and several gaseous species such as ozone, polycyclic aromatic hydrocarbons (PAHs), acetonitrile, benzene and isocyanic acid (Pudasainee et al., 2006; Aryal et al., 2009; Panday and Prinn, 2009; Sharma et al., 2012; World Bank, 2014; Chen et al., 2015; Putero et al., 2015: Sarkar et al., 2016). The ambient levels often exceed national air quality guidelines (Pudasainee et al., 2006; Aryal et al., 2009; Putero et al., 2015) and are comparable or higher than ambient levels observed in other major cities in South Asia.

Past studies in the Kathmandu Valley have focused mainly on a few aerosols species (BC, PM) and short-lived gaseous pollutants such as ozone and carbon monoxide (Pudasainee et al., 2006; Aryal et al., 2009; Panday and Prinn, 2009; Sharma et al., 2012, Putero et al., 2015). To the best of authors' knowledge, no direct measurements of CO_2 and CH_4 are available for the Kathmandu Valley. Recently, emission estimates of CO_2 and CH_4 were derived for the Kathmandu Valley using the International Vehicle Emission (IVE) model (Shrestha et al., 2013). The study estimated 1554 Gg of annual emission of CO_2 from a fleet of vehicles (that consisted of public buses, 3-wheelers, taxis and motor cycles; private cars, trucks and non-road vehicles were not included in the study) for the year 2010. In addition, the study also estimated 1.261 Gg of CH_4 emitted from 3 wheelers (10.6 %), taxis (17.7 %) and motorcycles (71 %) for 2010.

This study presents the first 12 months of measurements of two key GHGs, CH_4 and CO_2 along with other trace gases and meteorological parameters in Bode, a semi-urban site in the eastern part of the Kathmandu Valley. The year-long measurement in Bode is a part of the SusKat-ABC (Sustainable Atmosphere for the Kathmandu Valley – Atmospheric Brown Clouds) international air pollution measurement campaign conducted in and around the Kathmandu Valley from

December 2012 to June 2013. Details of the SusKat-ABC campaign are described in Rupakheti et al. (2017, manuscript in preparation). The present study provides a detailed account of seasonal and diurnal behaviors of CO_2 and CH_4 and their possible sources. To examine the rural-urban differences and estimate the urban enhancement, these gaseous species were also simultaneously measured for about three months (July - October) in 2015 at Chanban, a rural site about 25 km (aerial distance) outside and southwest of Kathmandu Valley. The seasonality of the trace gases and influence of potential sources in various (wind) directions are further explored by via ratio analysis. This measurement provides unique data from highly polluted but relatively poorly studied region (central Himalayan foothills in South Asia) which could be useful for validation of emissions estimates, model outputs and satellite observations. The study, which provides new insights on potential sources, can also be a good basis for designing mitigation measures for reducing emissions of air pollutants and controlling greenhouse gases in the Kathmandu Valley and the region.

2 Experiment and Methodology

2.1 Kathmandu Valley

The Kathmandu Valley consists of three administrative districts: Kathmandu, Lalitpur, and Bhaktapur, situated between 27.625° N, 27.75° N and 85.25° E, 85.375° E. It is a nearly circular bowl-shaped valley with a valley floor area of approximately 340 km^2 located at an altitude of 1300 meter above sea level (masl). The surrounding mountains are close to 2000-2800 m in height above sea level with five mountain passes located at about 200-600 m above the valley floor and an outlet for the Bagmati River southwest of the Kathmandu Valley. Lack of decentralization in in Nepal has resulted in the concentration of economic activities, health and education facilities, the service sector, as well as most of the central governmental offices in the Kathmandu Valley. Consequently, it is one of the fastest growing metropolitan areas in South Asia with a current population of about 2.5 million, and the population growth rate of 4 % per year (World Bank, 2013) Likewise, approximately 50 % of the total vehicle fleet (2.33 million) of the country is in Kathmandu Valley (DoTM, 2015). The consumption of fossil fuels such as liquefied petroleum gas (LPG), kerosene for cooking and heating dominates the residential

consumption, while the rest use biofuel (fuel wood, agro-residue, animal dung) for cooking and heating in the Kathmandu Valley. The commercial sector is also growing in the valley, and the latest data indicate the presence of 633 industries of various sizes. These are mainly associated with dyeing, brick kilns, and manufacturing industries. Fossil fuels such as coal and biofuels are the major fuels used in brick kilns. Brick kilns are reported as one of the major contributors of air pollution in the Kathmandu Valley (Chen et al., 2015; Kim et al., 2015; Sarkar et al., 2016). There are about 115 brick industries in the valley (personal communication with Mahendra Chitrakar, President of the Federation of Nepalese Brick Industries). Acute power shortage in the Valley is common all around the year, especially in the dry season (winter/pre-monsoon) when the power cuts can last up to 12 hours a day (NEA, 2014). Energy demand during the power cut period is met with the use of small (67 % of 776 generators surveyed for the World Bank study was with capacity less than 50 kVA) but numerous captive power generators (diesel/petrol), which further contribute to valley's poor air quality. According to the World Bank's estimate, over 250,000 such generator sets are used in the Kathmandu Valley alone, producing nearly 200 MW of captive power, and providing about 28 % of the total electricity consumption of the valley (World Bank, 2014). Apart from these sources, trash burning, which is a common practice (more prevalent in winter) throughout the valley, is one of the major sources of air pollutants and GHGs.

Climatologically, Kathmandu Valley has a sub-tropical climate with annual mean temperature of 18°C, and annual average rainfall of 1400 mm, of which 90 % occurs in monsoon season (June-September). The rest of the year is dry with some sporadic rain events. The wind circulation at large scale in the region is governed by the Asian monsoon circulation and hence the seasons are also classified based on such large scale circulations and precipitation: Pre-Monsoon (March-May), Monsoon (June-September), Post-Monsoon (October-November) and Winter (December-February). Sharma et al. (2012) used the same classification of seasons while explaining the seasonal variation of BC concentrations observed in the Kathmandu Valley. Locally in the valley, the mountain-valley wind circulations play an important role in influencing air quality. The wind speed at the valley floor is calm (≤ 1 m s^{-1}) in the morning and night, while a westerly wind develops after 11:00 in the morning till dusk, and switches to a mild easterly at night

198 (Panday and Prinn, 2009; Regmi et al., 2003). This is highly conducive to building up of air
199 pollution in the valley, which gets worse during the dry season.

200 **2.2 Study sites**

201 Two sites, a semi-urban site within the Kathmandu Valley and a rural site outside the Kathmandu
202 Valley, were selected for this study. The details of the measurements carried out in these sites is
203 described Table 1 and in section 2.2.1 and 2.2.2.

204 **2.2.1 Bode (SusKat-ABC supersite)**

205 The SusKat-ABC supersite was set up at Bode, a semi-urban location (Figure 1) of the
206 Madhyapur Thimi municipality in the Bhaktapur district in the eastern side of the Kathmandu
207 Valley. The site is located at 27.68° N latitude, 85.38° E longitude, and 1344 masl. The local
208 area around the site has a number of scattered houses and agricultural fields. The agriculture
209 fields are used for growing rice paddies in the monsoon season. It also receives outflow of
210 polluted air from three major cities in the valley: Kathmandu Metropolitan City and Lalitpur
211 Sub-metropolitan City, both mainly during daytime, and Bhaktapur Sub-metropolitan City
212 mainly during nighttime. Among other local sources around the site, about 10 brick kilns are
213 located in the east and southeast direction, approximately within 1-4 km from the site which are
214 operational only during dry season (January to April). There are close to 20 small and medium
215 industries (pharmaceuticals, plastics, electronics, tin, wood, aluminum, iron, fabrics etc.)
216 scattered in the same direction. The Tribhuvan International Airport (TIA) is located
217 approximately 4 km to the west of Bode.

218 **2.2.2 Chanban**

219 Chanban is a rural/background site in Makwanpur district outside of the Kathmandu Valley
220 (Figure 1). This site is located ~25 km aerial distance due southwest from Bode. The site is
221 located on a small ridge (27.65° N, 85.14° E, 1896 masl) between two villages - Chitlang and
222 Bajrabarahi - within the forested watershed area of Kulekhani Reservoir, which is located
223 approximately 4.5 km southwest of the site. The instruments were set up on the roof of 1-storey
224 building in an open space inside the Nepali Army barrack. There was a kitchen of the army

barrack at about 100 m to the southeast of the measurement site. The kitchen uses LPG, electricity, kerosene, and firewood for cooking activities.

2.3 Instrumentation

The measurements were carried out in two phases in 2013-2014 and 2015. In phase one, a cavity ring down spectrometer (Picarro G2401, USA) was deployed in Bode to measure ambient CO_2, CH_4, CO, and water vapor mixing ratios. Twelve months (6 March 2013 - 5 March 2014) of continuous measurements were made in Bode. The operational details of the instruments deployed in Bode are also provided in Table 1. In phase two, simultaneous measurements were made in Bode and Chanban for a little less than 3 months (15 July to 03 October 2015).

The Picarro G2401 analyzer quantifies spectral features of gas phase molecules by using a novel wavelength-scanned cavity ring down spectroscopic technique (CRDS). The instrument has a 30 km path length in a compact cavity that results in high sensitivity. Because of the high precision wavelength monitor, it uses absolute spectral position and maintains accurate peak quantification. Further, it only monitors the special features of interest to reduce drift. The instrument also has water correction to report dry gas fraction. The reported measurement precisions for CO_2, CH_4, CO and water vapor in dry gas is < 150 ppb, < 30 ppb, < 1 ppb and < 200 ppm for 5 seconds with 1 standard deviation (Picarro, 2015).

In Bode, the Picarro analyzer was placed on the 4^{th} floor of a 5-storey building with an inlet at 0.5 m above the roof of the building with a 360 degree view (total inlet height: 20 m above ground). The sample air was filtered at the inlet to keep dust and insects out and was drawn into the instrument through a 9 m Teflon tube (1/4 inch ID). The Picarro analyzer was set to record data every 5 second and recorded both directly sampled data and water corrected data for CO_2 and CH_4. In this paper, only water-corrected or dry mixing ratios of CH_4 and CO_2 were used to calculate the hourly averages for diurnal and seasonal analysis.

The instruments were factory calibrated before commencing the field measurements. Picarro G2401 model is designed for remote application and long term deployment with minimal drift and less requirement for intensive calibration (Crosson, 2008) and thus was chosen for the

current study in places like Kathmandu where there is no or limited availability of high quality reference gases. Regular calibration of Picarro G2401 in field during 2013-2014 deployment was not conducted due to challenges associated with the quality of the reference gas, especially for CO and CH_4. One time calibration was performed for CO_2 (at 395 and 895 ppm) in July 2015 before commencing the simultaneous measurements in Bode and Chanban in 2015. The difference between CO_2 mixing ratio reported by the analyzer and the reference mixing ratio was within 5 %. CO observations from Picarro G2401 were compared with observations from another CO analyzer (Horiba, model AP370) that was also operated in Bode for 3 months (March - May 2013). The Horiba CO monitor was a new unit, which was factory calibrated before its first deployment in Bode. Nevertheless, this instrument was inter-compared with another CO analyzer (same model) from the same manufacturer prior to the campaign and its correlation coefficient was 0.9 [slope of data from the new unit (y-axis) vs the old unit (x-axis) = 1.09]. Primary gas cylinders from Linde UK (1150 ppb) and secondary gases from Ultra-Pure Gases and Chemotron Science Laboratories (1790 ppb) were used for the calibration of CO instrument. Further details on CO measurements and calibration of Horiba AP370 can be found in Sarangi et al. (2014; 2016). A statistically significant correlation (r = 0.99, slope = 0.96) was found between Picarro and Horiba hourly average CO mixing ratio data (Supplementary Information Figure S1). Furthermore, the monthly mean difference between these two instruments (Horiba AP370 minus Picarro G2401) was calculated to be 0.02 ppm (3 %), 0.04 ppm (5 %) and 0.02 ppm (4 %) in March, April and May, respectively. For the comparison period of 3 months, the mean difference was 0.02 ppm (4 %). Overall differences were small to negligible during the comparison period and thus, adjustment in the data was deemed unnecessary.

Besides being highly selective to individual species, Picarro G2401 has a water correction function and thus accounts for the any likely drift in CO, CO_2 and CH_4 mixing ratios with the fluctuating water vapor concentration (Chen et al., 2013; Crosson, 2008). Crosson (2008) also estimated a peak to peak drift of 0.25 ppm. Further, Crosson (2008) observed a 1.2 ppb/day drift in CO_2 after 170 days from the initial calibration. For a duration of one year the drift will be less than 1 ppm, which is less than 1 % of the observed mixing ratio in (hourly ranges: 376-537 ppm)

Bode even if the drift was in same magnitude as in case of Crosson (2008). Crosson (2008) reported 0.8 ppb peak to peak drift in CH_4 measurements for 18 days after the initial calibration.

There were other instruments concurrently operated in Bode; a ceilometer for measuring mixing layer height (Vaisala Ceilometer CL31, Finland), and an Automatic Weather Station (AWS) (Campbell Scientific, USA). The ceilometer was installed on the rooftop (20 m above ground) of the building (Mues et al., 2017). For measuring the meteorological parameters, a Campbell Scientific AWS (USA) was set up on the roof of the building with sensors mounted at 2.9 m above the surface of the roof (22.9 m from the ground). The Campbell Scientific AWS measured wind speed and direction, temperature, relative humidity and solar radiation every minute. Temperature and rainfall data were taken from an AWS operated by the Department of Hydrology and Meteorology (DHM), Nepal at the Tribhuvan International Airport (TIA, see Figure 1), ~4 km due west of Bode site.

At Chanban, the inlet for Picarro gas analyzer was kept on the rooftop ~3 m above the ground and the sample air was drawn through a 3 m long Teflon tube (1/4 inches ID). The sample was filtered at the inlet with a filter (5-6 µm pore size) to prevent aerosol particles from entering into the analyzer. An AWS (Davis Vantage Pro2, USA) was also set up in an open area, about 17 m away from the building and with the sensors mounted at 2 m above ground.

3. Results and discussion

The results and discussions are organized as follow: Sub-section 3.1 describes a year round variation in CH_4, CO_2, CO and water vapor at Bode; sub-sections 3.2, 3.3 present the analysis of the observed monthly and seasonal variations and diurnal variation. Sub-sections 3.4 and 3.5 discuss the interrelation of CO_2, CH_4 and CO and potential emission sources in the valley and sub-section 3.6 compares and contrasts CH_4, CO_2, CO at Bode and Chanban.

3.1 Time series of CH_4, CO_2, CO and water vapor mixing ratios

Figure 2 shows the time series of hourly mixing ratios of CH_4, CO_2, CO, and water vapor at Bode. Meteorological data from Bode and the Tribhuvan International Airport are also shown in Figure 2. Data gaps in Figure 2a and 2b were due to maintenance of the measurement station. In

general, the fluctuations in the mixing ratio for CO were higher (in terms of % change) than in CH_4 and CO_2 during the sampling period. CO mixing ratios decreased and water vapor mixing ratios increased significantly during the rainy season (June-September). For the entire sampling period, the annual average (± one standard deviation) of CH_4, CO_2, CO, and water vapor mixing ratios were 2.192 (±0.066) ppm, 419.3 (±6.0) ppm, 0.50 (±0.23) ppm, and 1.73 (±0.66) %, respectively. The relative standard deviation (RSD) for the annual average of CH_4, CO_2 and CO were thus 3 %, 1.4 % and 46 %, respectively. The RSD at Mauna Loa were CH_4: 6 % and CO_2: 0.5 % and at Waliguan were CH_4: 0.48 %, CO_2: 0.9 %. The high variability in the annual mean, notably for CO in Bode could be indicative of the seasonality of emission sources and meteorology. The annual CH_4 and CO_2 mixing ratios were compared to the historical background site (Mauna Loa Observatory, Hawaii, USA) and the background site (Waliguan, China) in Asia, which will provide insight on spatial differences. The selection of neighboring urban and semi-urban sites, where many emission sources are typical for the region, for comparison provides information on relative differences (higher/lower), which will help in investigating possible local emission sources in the valley. As expected, annual mean of CH_4 and CO_2 mixing ratios in the Kathmandu Valley were higher than the levels observed at background sites in the region and elsewhere (Table 4). We performed a significance test at 95 % confidence level (t-test) of the annual mean values between the sites to evaluate whether the observed difference is statistically significant ($p < 0.05$), which was confirmed for the annual mean CH_4 and CO_2 between Bode and Mauna Loa, and between Bode and Waliguan. CH_4 was nearly 20 % higher at Bode than at Mauna Loa observatory (1.831 ± 0.110 ppm) (Dlugokencky et al., 2017) and calculated (ca.) 17 % higher than at Mt. Waliguan (1.879 ± 0.009 ppm) for the same observation period (Dlugokencky et al., 2016). The slightly higher CH_4 mixing ratios between at Bode and Waliguan than at Mauna Loa Observatory could be due to rice farming as a key source of CH_4 in this part of Asia. Thus, it could be associated with such agricultural activities in this region. Similarly, the annual average CH_4 at Bode during 2013-14 was found comparable to an urban site in Ahmedabad (1.880 ± 0.4 ppm, i.e., RSD: 21.3 %) in India for 2002 (Sahu and Lal, 2006) and 14 % higher than in Shadnagar (1.92 ± 0.07 ppm, i.e., RSD: 3.6 %), a semi-urban site in Telangana state (~70 km north from Hyderabad city) during 2014 (Sreenivas et al., 2016). Likewise, the difference between annual mean mixing ratios at Bode (419.3 ± 6.0 ppm, 1.4%

RSD) vs. Mauna Loa (396.8 ± 2.0 ppm, 0.5% RSD) and Bode vs. Waliguan (397.7 ± 3.6 ppm, 0.9% variability) (Dlugokencky et al., 2016a) was statistically significant ($p < 0.05$).

The high CH_4 and CO_2 mixing ratios at Bode in comparison to Ahmedabad and Shadnagar could be due to more than 115 coal-biomass fired brick kiln, some of them are located near the site (less than 4 km) and confinement of pollutants within the Valley due to bowl shaped topography of the Kathmandu Valley. Although Ahmedabad is a big city with high population larger than Kathmandu Valley, the measurement site is far from the nearby heavy polluting industries and situated in plains, where ventilation of pollutants would be more efficient as opposed to the Kathmandu Valley. The major polluting sources were industries, residential cooking and transport sector in Ahmedabad (Chandra et al., 2016). Shadnagar is a small town with a population of 0.16 million and major sources were industries (small-medium) and biomass burning in residential cooking (Sreenivas et al., 2016).

The monthly average of CO_2 mixing ratios in 2015 in Chanban (Aug: 403.4, Sep: 399.1 ppm) were slightly higher than the background sites at Mauna Loa Observatory (Aug: 398.89 ppm, Sep: 397.63 ppm) (NOAA, 2015) and Mt. Waliguan (Aug: 394.55 ppm, Sep: 397.68 ppm) (Dlugokencky et al., 2016a). For these two months in 2015, CH_4 mixing ratios were also higher in Bode (Aug: 2.281 ppm, Sep: 2.371 ppm) and Chanban (Aug: 2.050 ppm, Sep: 2.102 ppm) compared to Mauna Loa Observatory (Aug: 1.831 ppm, Sep: 1.846 ppm) (Dlugokencky et al., 2017)) and Mt. Waliguan (Aug: 1.915 ppm, 1.911 ppm) (Dlugokencky et al., 2016). The small differences in CO_2 between Chanban and background sites mentioned above indicate the smaller number of and/or less intense CO_2 sources at Chanban during these months because of the lack of burning activities due to rainfall in the region. The garbage and agro-residue burning activities were also absent or reduced around Bode during the monsoon period. However, high CH_4 values in August and September in Bode, Chanban and Mt. Waliguan in comparison to Mauna Loa Observatory may indicate the influence of CH_4 emission from paddy fields in the Asian region.

3.2 Monthly and Seasonal variations

Figure 3 shows the monthly box plot of hourly CH_4, CO_2, CO and water vapor observed for a year in Bode. Monthly and seasonal averages of CH_4 and CO_2 mixing ratios at Bode are summarized in Table 2 and 3. CH_4 were lowest during May-July (ranges from 2.093-2.129 ppm) period and highest during August-September (2.274-2.301 ppm), followed by winter. In addition to the influence of active local sources, the shallow boundary layer in winter was linked to elevated concentrations (Panday and Prinn, 2009; Putero et al., 2015, Mues et al., 2017). The low CH_4 values from May to July may be associated with the absence of brick kiln and frequent rainfall in these months. Brick kiln were operational during January to April. Rainfall also leads to suppression of open burning activities in the valley (see Figure 2b). The CH_4 was slightly higher (statistically significant, $p < 0.05$) in monsoon season (July–September) than in the pre-monsoon season (unlike CO_2 which was higher in pre-monsoon), and could be associated with the addition of CH_4 flux from the water-logged rice paddies (Goroshi et al., 2011). There was a visible drop in CH_4 from September to October but remained consistently over 2.183 ppm from October to April with little variation between these months. Rice-growing activities are minimal or none in October and beyond, and thus may be related to the observed dip in CH_4 mixing ratio.

Comparison of seasonal average CH_4 mixing ratios at Bode and Shadnagar (a semi-urban site in India) indicated that CH_4 mixing ratios at Bode were higher in all seasons than at Shadnagar: pre-monsoon (1.89 ± 0.05 ppm), monsoon (1.85 ± 0.03 ppm), post-monsoon (2.02 ± 0.01 ppm), and winter (1.93 ± 0.05 ppm) (Sreenivas et al., 2016). The possible reason for lower CH_4 at Shadnagar in all seasons could be associated with geographical location and difference in local emission sources. The highest CH_4 mixing ratio in Shadnagar was reported in post-monsoon which was associated with harvesting in the Kharif season (July – October), while the minimum was in monsoon. Shadnagar is a relatively small city (population: ~0.16 million) compared to Kathmandu Valley and the major local sources which may have influence on CH_4 emissions include bio-fuel, agro-residue burning and residential cooking.

The seasonal variation in CO_2 could be due to (i) the seasonality of major emission sources such as brick kilns (ii) seasonal growth of vegetation (CO_2 sink) (Patra et al., 2011) and (iii) atmospheric transport associated with regional synoptic atmospheric circulation (monsoon circulation and westerly disturbance in spring season) which could transport regional emission

sources from vegetation fire and agriculture residue burning (Putero et al., 2015), and a local mountain-valley circulation effect (Kitada and Regmi, 2003; Panday et al., 2009). The concentrations of most pollutants in the region are lower during the monsoon period (Sharma et al., 2012, Marinoni, 2013; Putero et al., 2015) because frequent and heavy rainfall suppresses emissions sources. We saw a drop in the CO_2 mixing ratio during the rainfall period due to changes in various processes such as enhanced vertical mixing, uptake of CO_2 by vegetation and soils, and, where relevant, reduction in combustion sources. CO_2 can also dissolve into rainfall, forming carbonic acid, which may lead to a small decrease in the CO_2 mixing ratio as has been observed during high intensity rainfall (Chaudhari et al., 2007; Mahesh et al., 2014). Monsoon is also the growing season with higher CO_2 assimilation by plants than other seasons (Sreenivas et al., 2016). In contrast, winter, pre-monsoon and post-monsoon season experiences an increase in emission activities in the Kathmandu Valley (Putero et al., 2015).

The CO_2 mixing ratios were in the range of 376 - 537 ppm for the entire observation period. Differences with CH_4 were observed in September and October where CO_2 was increasing (mean/median) in contrast to CH_4 which showed the opposite trend. The observed increase in CO_2 after October may be related to little or no rainfall, which results in the absence of rain-washout and/or no suppression of active emission sources such as open burning activities. However, the reduction in CH_4 after October could be due to reduced CH_4 emissions from paddy fields, which were high in August-September. CO_2 remains relatively low during July-August, but it is over 420 ppm from January to May. Seasonal variation of CO_2 in Bode was similar in seasonal variation but the values are higher than the values observed in Shadnagar, India (Sreenivas et al., 2016).

The variations in CO were more distinct than CH_4 and CO_2 during the observation period (Figure 3). The highest CO values were observed from January-April (0.71-0.91 ppm). The seasonal mean of CO mixing ratios at Bode were: pre-monsoon (0.60 ± 0.36 ppm), monsoon (0.26 ± 0.09 ppm), post-monsoon (0.40 ± 0.15 ppm), and winter (0.76 ± 0.43 ppm). The maximum CO was observed in winter, unlike CO_2 which was maximum in pre-monsoon. The high CO in winter was due to the presence of strong local pollution sources (Putero et al., 2015)

and shallow mixing layer heights. The addition of regional forest-fire and agro-residue burning augmented CO_2 mixing ratios in pre-monsoon. The water vapor mixing ratio showed a seasonal pattern opposite of CO, with a maximum in monsoon (2.53 %) and minimum in winter (0.95 %), and intermediate values of 1.56 % in pre-monsoon and 1.55 % in post-monsoon season.

There were days in August-September when the CH_4 increased by more than 3 ppm (Figure 2). Enhancement in CO_2 was also observed during the same time period. In the absence of tracer model simulations, the directionality of the advected air masses is unclear. Figure 4 shows that during these two months, CO_2 mixing rations were particularly high (> 450 CO_2 and > 2.5 ppm CH_4) with the air masses coming from the East-Northeast (E-NE). CO during the same period was not enhanced and didn't show any particular directionality compared to CH_4 and CO_2 (Figure 4c). Areas E-NE to Bode are predominantly irrigated (rice paddies) during August-September, and sources such as brick kilns were not operational during this time period. Goroshi et al. (2011) reported that June to September is a growing season for rice paddies in South Asia with high CH_4 emissions during these months and observed a peak in September in the atmospheric CH_4 column over India. Model analysis also points to high methane emissions in September which coincides with the growing period of rice paddies (Goroshi et al., 2011, Prasad et al., 2014). The CH_4 mixing ratios at Bode in January (2.233 ± 0.219 ppm) and July (2.129 ± 0.168 ppm) were slightly higher than the observation in Darjeeling (Janurary: 1.929 ± 0.056 ppm; July: 1.924 ± 0.065 ppm), a hill station of eastern Himalaya (Ganesan et al., 2013). The higher CH_4 values in January and July at Bode compared to Darjeeling could be because of the influence of local sources, in addition to the shallow boundary layer in Kathmandu Valley. Trash burning and brick kilns are two major sources from December until April in the Kathmandu Valley while emission from paddy fields occurs during July-September in the Kathmandu Valley. In contrast, the measurement site in Darjeeling was located at higher altitude (2194 masl) and was less influenced by the local emission. The measurement in Darjeeling reflected a regional contribution. There are limited local sources in Darjeeling such as wood biomass burning, natural gas related emission and vehicular emission (Ganesan et al., 2013).

The period between January and April had generally higher or the highest values of CO_2, CH_4 and CO at Bode. The measurement site was impacted mainly by local Westerly-Southwesterly

winds (W-SW) and East-Southeast (E-SE). The W-SW typically has a wind speed in the range ~1 - 6 m s^{-1} and was active during late morning to afternoon period (~11:00 to 17:00 NST, supplementary information Figure S2 and S3). Major cities in the valley such as Kathmandu Metropolitan City and Lalitpur Sub-metropolitan City are W-SW of Bode (Figure 1c). Wind from E-SE were generally calm ($\leq$1 m s^{-1}) and observed only during night and early morning hours (21:00 to 8:00 NST). The mixing ratio of all three species in air mass from the E-SE was significantly higher than in the air mass from W-SW (Figure 4). There are 10 biomass co-fired brick kilns and Bhaktapur Industrial Estate located within 1-4 km E-SE from Bode (Sarkar et al., 2016). The brick kilns were only operational during January-April. Moreover, there were over 100 brick kilns operational in the Kathmandu Valley (Putero et al., 2015) which use low-grade lignite coal imported from India and biomass fuel to fire bricks in inefficient kilns (Brun, 2013).

Fresh emissions from the main city center were transported to Bode during daytime by W-SW winds which mainly include vehicular emission. Compared to monsoon months (June-August), air mass from W-SW had higher values of all three species (Figure 4) during winter and pre-monsoon months. This may imply that in addition to vehicular emission, there are other potential sources which were exclusively active during these dry months. Municipal trash burning is also common in the Kathmandu Valley, with a reported higher frequency from December to February (Putero et al., 2015). The frequency in the use of captive power generator sets are highest during the same period, which is another potential source contributing to air coming from W-SW direction (World Bank, 2014; Putero et al., 2015).

Regional transport of pollutants into the Kathmandu Valley was reported by Putero et al. (2015). To relate the influence of synoptic circulation with the observed variability in BC and O_3 in the Kathmandu Valley, 5-day back trajectories (of air masses arriving in the Kathmandu Valley) were computed by Putero et al., (2015) using the HYSPLIT model. These individual trajectories which were initialized at 600 hPa, for the study period of one year and were clustered into nine clusters. Of the identified clusters, the most frequently observed clusters during the study period were the Regional and Westerly cluster or circulation (22 % and 21 %). The trajectories in the regional cluster originate within 10^o x 10^o around the Kathmandu Valley, whereas the majority of trajectories in this westerly cluster originated broadly around 20-40^0 N, ~60^0 E. Putero et al

(2015) found that the regional and westerly synoptic circulation were favorable for high values of BC and O_3 in the Kathmandu Valley. Other sources of CO_2 and CH_4 could be due to vegetation fires which were also reported in the region surrounding the Kathmandu Valley during the pre-monsoon months (Putero et al., 2015). Similarly, high pollution events, peaking in the pre-monsoon, were observed at Nepal Climate Observatory-Pyramid (NCO-P) near Mt. Everest, which have been associated with vegetation fires in the Himalayan foothills and northern IGP region (Putero et al., 2014). MODIS derived forest counts (Figure 5), which also indicated high frequency of forest fire and farm fires from February to April and also during post-monsoon season. It is interesting that the monthly mean CO_2 mixing ratio was maximum in April (430 ± 27 ppm) which could be linked to the fire events. It is likely that the westerly winds (> 2.5 - 4.5 m s^{-1}) during the daytime (supplementary information Figure S2, S3) bring additional CO_2 from vegetation fires and agro-residue burning in southern plains of Nepal including the IGP region (Figure 5). Low values of CO_2 and CH_4 during June-July (Figure 3) were coincident with the rainy season, and sources such as brick kiln emission, trash burning, captive power generators, and regional agriculture residue burning and forest fires are weak or absent during these months.

3.3 Diurnal Variation

Figure 6 shows the average seasonal diurnal patterns of CH_4, CO_2, CO, and water vapor mixing ratios observed at Bode for four seasons. All the three gas species had a distinct diurnal patterns in all seasons, characterized by maximum values in the morning hours (peaked around 7:00-9:00), afternoon minima around 15:00-16:00, and a gradual increase through the evening until next morning. There was no clear evening peak in CH_4 and CO_2 mixing ratios whereas CO shows an evening peak around 20:00. The gradual increase of CO_2 and CH_4 in the evening in contrast to the increase until evening peak traffic hours and later decay of CO may be indicative of a few factors. As pointed out earlier, after the peak traffic hours, there are no particularly strong sources of CO, especially in the monsoon and post-monsoon season. It is also likely that some of the CO is decayed due to nighttime katabatic winds which replace polluted air masses with cold and fresh air from the nearby mountain (Panday and Prinn, 2009). As for the CO_2, the biosphere respiration at night in the absence of photosynthesis can add additional CO_2 to the

atmosphere which especially in the very shallow nocturnal boundary layer may explain part of the increase of the CO_2 mixing ratio. The well-defined morning and evening peaks observed in CO mixing ratios are associated with the peaks in traffic and residential activities. The CH_4 and CO_2 showed pronounced peaks in the morning hours (07:00 - 09:00) in all seasons with almost the same level of seasonal average mixing ratios. CO had a prominent morning peak in winter and pre-monsoon season, but the peak was significantly lower in monsoon and post-monsoon. The CO (~1 - 1.4 ppm) around 08:00 - 09:00 in winter and pre-monsoon were nearly 3-4 times higher than in monsoon and post-monsoon season. It appears that CH_4 and CO_2 mixing ratios were continuously building up at night until the following morning peak in all seasons. The similar seasonal variations in CH_4 and CO_2 across all seasons could be due to their long-lived nature, as compared to CO, whose diurnal variations are strongly controlled by the evolution of the boundary layer. Kumar et al. (2015) also reported morning and evening peaks and an afternoon low in CO_2 mixing ratios in industrial, commercial, and residential sites in Chennai in India. The authors also found high early morning CO_2 mixing ratios at all sites and attributed it to the temperature inversion and stable atmospheric condition.

The daytime low CH_4 and CO_2 mixing ratios were due to (i) elevated mixing layer height in the afternoon (Figure 7), (ii) development of upslope wind circulation in the valley, and (iii) development of westerly and southwesterly winds which blows through the valley during the daytime from around 11:00 to 17:00 (supplementary information Figure S2), all of which aid in dilution and ventilation of the pollutants out of the valley (Regmi et al., 2003; Kitada and Regmi, 2003; Panday and Prinn, 2009). In addition, the daytime CO_2 minimum in the summer monsoon is also associated with high photosynthetic activities in the valley as well as in the broader surrounding region. In the nighttime and early morning, the mixing layer height was low (only around 200-300 m in all seasons) and remains stable for almost 17 hours a day. In the daytime it grows up to 800-1200 m for a short time (ca. from 11:00 to 18:00) (Mues et al., 2017). Therefore the emissions from various activities in the evening after 18:00 (cooking and heating, vehicles, trash burning, and bricks factories in the night and morning) were trapped within the collapsing and shallow boundary layer, and hence mixing ratios were high during evening, night and morning hours. Furthermore, plant and soil respiration also increases CO_2 mixing ratio during

the night (Chandra et al., 2016). However, Ganesan et al. (2013) found a distinct diurnal cycle of CH_4 mixing ratios with twin peaks in the morning (7:00 - 9:00), and afternoon (15:00 - 17:00) and a nighttime low in winter but no significant diurnal cycle in the summer of 2012 in Darjeeling, a hill station (2194 masl) in the eastern Himalaya. The authors described that the morning peaks could be due to the radiative heating of the ground in the morning, which breaks the inversion layer formed during night, and as a result, pollutants are ventilated from the foothills up to the site. The late afternoon peaks match wind direction and wind speed (upslope winds) that could bring pollution from the plains to the mountains.

The diurnal variation of CO is also presented along with CO_2 and CH_4 in Figure 6c. CO is an indicator of primary air pollution. Although the CO mixing ratio showed distinct diurnal pattern, it was different from the diurnal patterns of CO_2 and CH_4. CO diurnal variation showed distinct morning and evening peaks, afternoon minima, and a nighttime accumulation or decay. Nighttime accumulation in CO was observed only in winter and pre-monsoon and decay or decrease in monsoon season and post-monsoon season (Figure 7). The lifetime of CO (weeks to months) is very long compared to the ventilation timescales for the valley, so the different diurnal cycles would be due to differences in nighttime emissions. While the biosphere respires at night which may cause a notable increase in CO_2 in the shallow boundary layer, most CO sources (transport sector, residential cooking) except brick kilns remain shut down or less active at night. This also explains why nighttime values of CO drop less in the winter and pre-monsoon than in other seasons. Furthermore, the prominent morning peaks of CO in pre-monsoon and winter compared to other seasons results from nighttime accumulation, additional fresh emissions in the morning and recirculation of the pollutants due to downslope katabatic winds (Pandey and Prinn, 2009; Panday et al., 2009). Pandey and Prinn (2009) observed nighttime accumulation and gradual decay during the winter (January 2005). The measurement site in Pandey and Prinn (2009) was near the urban core of the Kathmandu Valley and had significant influence from the vehicular sources all over the season including the winter season. Bode lies in close proximity to the brick kilns which operate 24 hours during the winter and pre-monsoon period. Calm southeasterly winds are observed during the nighttime and early morning (ca. 22:00

– 8:00) in pre-monsoon and winter, which transport emissions from brick kiln to the site (Sarkar et al., 2016). Thus the gradual decay in CO was not observed in Bode.

The timing of the CO morning peak observed in this study matches with observations by Panday et al. (2009). They also found CO morning peak at 8:00 in October 2004 and at 9:00 in January 2005. The difference could be linked to the boundary layer stability. As the sun rises later in winter, the boundary layer stays stable for a longer time in winter keeping mixing ratios higher in morning hours than in other seasons with an earlier sunrise.

The morning peaks of CO_2 and CH_4 mixing ratios occurred around 6:00 -7:00 local time in the pre-monsoon, monsoon, and post monsoon season, whereas in winter their peaks are delayed by 1-2 hours in the morning; CH_4 at 8:00 and CO_2 at 9:00. The CO showed that its morning peak was delayed compared to CO_2 and CH_4 morning peaks by 1-2 hour in pre-monsoon, monsoon and post-monsoon (at 8:00) and in winter (at 9:00). The occurrence of morning peaks in CO_2 and CH_4 1-2 hours earlier than CO is interesting. This could be due to the long lifetimes and relatively smaller local sources of CH_4 and CO_2, as CO is mainly influenced by emissions from vehicles during rush hour, as well as from biomass and trash burning in the morning hours. Also, CO increases irrespective of change in the mixing layer (collapsing or/rising, Figure 7) but CO_2 and CH_4 start decreasing only after the mixing layer height starts to rise. Recently, Chandra et al. (2016) also reported that the CO_2 morning peak occurred earlier than CO in observations in Ahmedabad City India. This was attributed to CO_2 uptake by photosynthetic activities after sunrise but CO kept increasing due to emissions from the rush hour activities.

The highest daytime minimum of CO_2 was observed in the pre-monsoon followed by winter (Figure 6b). The higher daytime minimum of CO_2 mixing ratios in the pre-monsoon season than in other seasons, especially winter, is interesting. The local emission sources are similar in pre-monsoon and winter and the boundary layer is higher (in the afternoon) during the pre-monsoon (~1200 m) than in winter (~900 m) (Mues et al., 2017). Also, the biospheric activity in the region is reported to be higher in the pre-monsoon (due to high temperature and solar radiation) than winter (Rodda et al., 2016). Among various possible causes, transport of CO_2 rich air from outside the Kathmandu Valley has been hypothesized as a main contributing factor, due to

regional vegetation fires combined with westerly mesoscale to synoptic transport Putero et al. (2015). In monsoon and post-monsoon seasons, the minimum CO_2 mixing ratios in the afternoon drops down to 390 ppm, this was close to the values observed at the regional background sites Mauna Loa and Waliguan.

3.4 Seasonal interrelation of CO_2, CH_4 and CO

The Pearson's correlation coefficient (r) between CO_2 and CO was strong in winter (0.87), followed by monsoon (0.64), pre-monsoon (0.52) and post-monsoon (0.32). The higher coefficient in winter indicates that common or similar sources for CO_2 and CO and moderate values in pre-monsoon and monsoon indicates the likelihood of different sources. To avoid the influence of strong diurnal variations observed in the valley, daily averages, instead of hourly, were used to calculate the correlation coefficients. The correlation coefficients between daily CH_4 and CO_2 for four seasons are as follows: winter (0.80), post-monsoon (0.74), pre-monsoon (0.70) and monsoon (0.22). A semi-urban measurement study in India also found a strong positive correlation between CO_2 and CH_4 in the pre-monsoon (0.80), monsoon (0.61), post-monsoon (0.72) and winter (0.8) (Sreenivas et al., 2016). It should be noted here that Sreenivas et al., (2006) used hourly average CO_2 and CH_4 mixing ratios. The weak monsoon correlation at Bode, which is in contrast to Sreenivas et al. (2016), may point to the influence of dominant CH_4 emission from paddy field during the monsoon season (Goroshi et al., 2011). Daily CH_4 and CO was also weakly correlated in monsoon (0.34) and post-monsoon (0.45). Similar to CH_4 and CO_2, the correlation between CH_4 and CO were moderate to strong in pre-monsoon (0.76) and winter (0.75).

Overall, the positive and high correlations between CH_4 and CO mixing ratios and between CH_4 and CO_2 mixing ratios in the pre-monsoon and winter indicate common sources, most likely combustion related sources such as vehicular emission, brick kilns, agriculture fire etc., or the same source regions (i.e. their transport due to regional atmospheric transport mechanisms). Weak correlation, between CH_4-CO_2 and between CH_4-CO, during monsoon season indicates sources other than combustion-related may be active, such as agriculture as a key CH_4 source (Goroshi et al., 2013)

3.5 CO and CO_2 ratio: Potential emission sources

The ratio of the ambient mixing ratios of CO and CO_2 was used as an indicator to help discriminate emission sources in the Kathmandu Valley. The ratio was calculated from the excess (dCO and dCO_2) relative to the background values of ambient CO and CO_2 mixing ratios. The excess value was estimated by subtracting the base value which was calculated as the fifth percentile of the hourly data for a day (Chandra et al., 2016).

Average emission ratios from the literature are shown in Table 5, and average ratios of dCO/dCO_2 are shown in Table 6, disaggregated into morning hours, evening hours, and seasonal values. It must be stated that due to the large variance in the calculated ratio from this study (Table 6) as well as the likely variation in the estimated ratio presented in Table 5, the interpretation and conclusion about sources should be cautiously drawn and will be indicative. Higher ratios were found in pre-monsoon (12.4) and winter (15.1) season compared to post-monsoon (8.3) and monsoon (7.5). These seasonal differences in the dCO/dCO_2 ratio are depicted in Figure 8, which shows a clear relationship with the wind direction and associated emissions, with the highest values especially for stronger westerly winds. Compared to the other three seasons, the ratio in winter was also relatively high for air masses from the east, likely due to emissions from brick kilns combined with accumulation during more stagnant meteorological conditions (supplementary information Figure S2, S3). In other seasons, emission emanating from the north and east of Bode were characterized by a dCO/dCO_2 ratio below 15. Air masses from the west and south generally have a ratio from 20 to 50 in all but post-monsoon season, where the ratio sometimes exceeds 50. A ratio of 50 or over is normally due to very inefficient combustion sources (Westerdahl et al., 2009; Stockwell et al., 2016), such as agro-residue burning, which is common during the post-monsoon season in the Kathmandu Valley.

For interpretability of emission ratio with sources, the ratio was classified into three categories: (i) 0 – 15, (ii) 15 – 45, and (iii) greater than 45. This classification was based on the observed distribution of emission ratio during the study period (Figure 8) and a compilation of observed emission ratios typical for different sources from Nepal and India (see Table 5). An emission ratio below 15 is likely to indicate residential cooking and diesel vehicles, and captive power

generation with diesel-powered generator sets (Smith et al., 2000; ARAI, 2008; World Bank, 2014). The emission from brick kilns (FCBTK and Clamp kilns, both common in the Kathmandu Valley), and inefficient, older (built before 2000) gasoline cars fall in between 15 - 45 (ARAI, 2008; Weyant et al., 2014; Stockwell et al., 2016). Four-stroke motorbikes and biomass burning activities (mixed garbage, crop-residue and biomass) are one of the least efficient combustion sources, with emission ratios higher than 45 (ARAI, 2008; Westerdahl et al., 2009; Stockwell et al., 2016).

Although ratio of dCO/dCO_2 is a weak indicator of sources and the mean ratio has large variance (See Table 6), the conclusions drawn, from using Figure 8 and the above mentioned classification, are not conclusive. The estimated dCO/dCO_2 ratio tentatively indicates that the local plume impacting the measurement site (Bode) from the north and east could be residential and/or diesel combustion. The estimated dCO/dCO_2 ratio of the local plume from the south and west generally falls in the 15-45 range which could indicate emissions from brick kilns and inefficient gasoline vehicles. Very high ratios were also estimated from the south west during the post-monsoon season. Among other possible sources, this may indicate agro-residue open burning.

The emission inventory for CO identifies (aggregate for a year) residential, and gasoline related emission from transport sector (Sadavarte et al., 2017, in preparation*)*. The inventory is not yet temporally resolved, so no conclusion can be drawn about the sources with respect to different seasons. From the 1 km x 1 km emission inventory of the Kathmandu Valley for 2011, the estimated sectoral source apportionment of CO is residential (37 %), transport sector (40 %) and industrial (20 %). The largest fraction from the residential sector is cooking (24 %) whereas the majority of transport sector related CO in the Kathmandu Valley is from gasoline vehicles.

The dCO/dCO_2 ratio also changes markedly between the morning peak hours (07:00-09:00, except in winter season when the peak occurs during 08:00-09:00) and evening peak hours (19:00-21:00 pm) (Table 6). Morning and evening values were lowest (2.2, 8.0) during the monsoon and highest (11.2, 21.6) in the winter season, which points to the different emission characteristics in these two seasons. This feature is similar to Ahmedabad, India, another urban

site in south Asia, where the morning/evening values were lowest (0.9/19.5) in monsoon and highest in winter (14.3/47.2) (Chandra et al., 2016). In the morning period, the ratio generally falls within a narrower range, from less than 1 to about 25, which indicates a few dominant sources, such as cooking, diesel vehicles, and diesel gen-sets (see Figure 9). In the evening period, the range of the ratio is much wider, from less than 1 to more than 100, especially in winter. This is partly due to the shallower boundary layer in winter, giving local CO emissions a chance to build up more rapidly compared to the longer-lived and well-mixed CO_2, and also indicating the prevalence of additional sources such as brick kilns and agro-residue burning.

3.6 Comparison of CH_4 and CO_2 at semi-urban site (Bode) and rural site (Chanban)

Figure 10 shows time series of hourly average mixing ratios of CH_4, CO_2, CO and water vapor observed simultaneously at Bode and Chanban for the period of 15th July to 3rd October 2015. The hourly meteorological parameters observed at Chanban are shown in supplementary Figure S4. The hourly temperature ranges from 14 to 28.5° C during the observation period. The site experienced calm winds during the night and moderate southeasterly winds with hourly maximum speed of up to 7.5 m s^{-1} during the observation period. The CH_4 mixing ratios at Chanban varied from 1.880 ppm to 2.384 ppm, and generally increased from the last week of July until early September, peaking around 11th September and then falling off towards the end of the month. CO followed a generally similar pattern, with daily average values ranging from 0.10 ppm to 0.28 ppm. The hourly CO_2 mixing ratios ranged from 375 to 453 ppm, with day to day variations, but there were no clear pattern as observed in trend like CH_4 and CO mixing ratios.

The CH_4, CO_2, and CO mixing ratios were higher in Bode than in Chanban (Figure 10, Table 4), with Chanban approximately representing the baseline of the lower envelope of the Bode levels. The mean CO_2, CH_4 and CO mixing ratios over the entire sampling period of nearly three months at Bode are 3.8 %, 12.1 %, and 64 % higher, respectively, than at Chanban. The difference in the CO_2 mixing ratio could be due to the large uptake of CO_2 in the forested area at Chanban and surrounding regions compared to Bode, where the local anthropogenic emissions rate is higher and less vegetation for photosynthesis. The coincidence between the base values of

CO and CH_4 mixing ratios at Bode and the levels observed at Chanban implies that Chanban CO and CH_4 mixing ratios are indicative of the regional background levels. A similar increase in CO and CH_4 mixing ratios at Chanban from July to September was also observed at Bode, which may imply that the regional/background levels in the broader Himalayan foothill region also influences the baseline of the daily variability of the pollutants in the Kathmandu Valley, consistent with Panday and Prinn (2009).

Figure 11 shows the comparison of average diurnal cycles of CO_2, CH_4, CO and water vapor mixing ratios observed at Bode and Chanban. The diurnal pattern of CO_2 mixing ratios at both sites is similar, but more pronounced at Bode, with a morning peak around 06:00-07:00, a daytime minimum, and a gradual increase in the evening until the next morning peak. A prominent morning peak at Bode during the monsoon season indicates the influence of local emission sources. The daytime CO_2 mixing ratios are also higher at Bode than at Chanban because of local emissions less uptake of CO_2 for photosynthesis in the valley in comparison to the forested area around Chanban. Like the diurnal pattern of CO_2 depends on the evolution of the mixing layer at Bode, as discussed earlier, it is expected that the mixing layer evolution similarly influences the diurnal CO_2 mixing ratios at Chanban. CO, on the other hand, shows very different diurnal patterns at Bode and Chanban. Sharp morning and evening peaks of CO are seen at Bode, indicating the strong local polluting sources, especially cooking and traffic in the morning and evening peak hours. Chanban, in contrast, only has a subtle morning peak and no evening peak. After the morning peak, CO sharply decreases at Bode but not at Chanban. The growth of the boundary layer after sunrise and entrainment of air from the free troposphere, with lower CO mixing ratios, causes CO to decrease sharply during the day at Bode. At Chanban, on the other hand, since the mixing ratios are already more representative of the local and regional background levels which will also be prevalent in the lower free troposphere, CO does not decrease notably during the daytime growth of the boundary layer as observed at Bode.

Similarly, while there is very little diurnal variation in the CH_4 mixing ratios at Chanban, there is a strong diurnal cycle of CH_4 at Bode, similar to CO_2 there. At Chanban, the CH_4 mixing ratio only shows a weak minimum at around 11:00, a slow increase during the day until a its peak around 22:00, followed by a slow decrease during the night and a more rapid decrease through

739 the morning. The cause of this diurnal pattern at Chanban is presently unclear, but the levels
740 could be representative of the regional background throughout the day and show only limited
741 influences of local emissions.
742
743 4. **Conclusions**

744 A cavity ring down spectrometer (Picarro G2401, USA) was used to measure ambient CO_2, CH_4,
745 CO, and water vapor mixing ratios at a semi-urban site (Bode) in the Kathmandu Valley for a
746 year. This was the first 12-months of continuous measurements of these four species in the
747 Kathmandu Valley in the foothills of the central Himalaya. Simultaneous measurement was
748 carried out at a rural site (Chanban) for approximately 3 months to evaluate urban-rural
749 differences.

750 The measurement also provided an opportunity to establish diurnal and seasonal variation of
751 these species in one of the biggest metropolitan cities in the foothills of Himalayas. Annual
752 average of the mixing ratio of CH_4 and CO_2 in Bode revealed that they were higher than the
753 mixing ratios at the background sites such as the Mauna Loa, USA and Mt. Waliguan, China, as
754 well as higher than urban/semi-urban sites in nearby regions such as Ahmedabad and Shadnagar
755 in India. These comparisons highlight potential sources of CH_4 and CO_2 in the Kathmandu
756 Valley, such as brick kilns in the valley.

757 Polluted air masses were transported to the site mainly by two major local wind circulation
758 patterns, East-South and North-East and West-Southwest throughout the observation period.
759 Strong seasonality was observed with CO compared to CO_2 and CH_4. Winter and pre-monsoon
760 high CO are linked to emission sources active in these seasons only and are from east-southeast
761 and west-southwest. Emission from the east-southeast are most likely related to brick kilns
762 (winter and pre-monsoon), which are in close proximity to Bode. Major city-centers are located
763 in the west-southwest of Bode (vehicular emission) which impact the site all-round the year,
764 although higher during winter season. Winter high was also observed with CO_2 and CH_4, which
765 are mostly local influence of brick kilns, trash burning and emission from city-center. Nighttime
766 and early morning accumulation of pollutants in winter due to a shallow stable mixing height (ca.

200 m) also contribute to elevated levels than other seasons. Diurnal variation across all seasons indicates the influence of rush-hour emissions related to vehicles and residential emissions. The evolution of the mixing layer height (200 -1200 m) was a major factor which controls the morning-evening peak, afternoon low and night-early morning accumulation or decay. Thus the geographical setting of the Kathmandu Valley and its associated meteorology play a key role in the dispersion and ventilation of pollutants in the Kathmandu Valley. The ratio of dCO/dCO_2 across different seasons and wind directions suggested that emissions from inefficient gasoline vehicles, brick kilns, residential cooking and diesel combustion are likely to impact Bode.

The differences in mean values for urban-rural measurements at Bode and Chanban is highest for CO (64 %) compared to CO_2 (3.8 %) and CH_4 (12 %). Low values of CH_4 and CO_2 mixing ratios at the Chanban site could represent ~~a~~ regional background mixing ratios.

This study has provided valuable information on key greenhouse gases and air pollutants in the Kathmandu Valley and the surrounding regions. These observations can be useful as ground-truthing for evaluation of satellite measurements, as well as climate and regional air quality models. The overall analysis presented in the paper will contribute along with other recent measurement and analysis to providing a sound scientific basis for reducing emissions of greenhouse gases and air pollutants in the Kathmandu Valley.

Acknowledgements

The IASS is grateful for its funding from the German Federal Ministry for Education and Research (BMBF) and the Brandenburg Ministry for Science, Research and Culture (MWFK). This study was partially supported by core funds of ICIMOD contributed by the governments of Afghanistan, Australia, Austria, Bangladesh, Bhutan, China, India, Myanmar, Nepal, Norway, Pakistan, Switzerland, and the United Kingdom as well as funds provided to ICIMOD's Atmosphere Initiative by the Governments of Sweden and Norway. We are thankful to Bhogendra Kathayat, Shyam Newar, Dipesh Rupakheti, Piyush Bhardwaj, Ravi Pokharel, and Pratik Singdan for their assistance during the measurement, P.S. Praveen for his support in calibration of Picarro instrument, Pankaj Sadavarte for his help in refining Figure 1, and Liza

Manandhar and Rishi KC for the logistical support. The authors also express their appreciation to the Department of Hydrology and Meteorology (DHM), Nepal, and the Nepal Army.

References

Aryal, R. K., Lee, B.-K., Karki, R., Gurung, A., Baral, B., and Byeon, S.-H.: Dynamics of PM 2.5 concentrations in Kathmandu Valley, Nepal, J.~~ournal of~~ H~~h~~azard.~~ous~~ M~~m~~at.~~erials~~, 168, 732-738, 2009.

Automotive Research Association of India (ARAI).: Emission factor development for Indian vehicles (http://www.cpcb.nic.in/Emission_Factors_Vehicles.pdf), 2008.

Brun, V. (Eds. 1): Fried earth bricks, kilns and workers in Kathmandu Valley. Himal Books, Lazimpat-Kathmandu, Nepal, 2013.

Central Bureau of Statistics (CBS).: Nepal Living Standards Survey 2010/11, Statistical Report Volume 1, Central Bureau of Statistics, Government of Nepal, 2011.

Chandra, N., Lal, S., Venkataramani, S., Patra, P. K., and Sheel, V.: Temporal variations of atmospheric CO 2 and CO at Ahmedabad in western India, Atmos. Chem. Phys., 16, 6153-6173, 2016.

Chen, H., Karion, A., Rella, C., Winderlich, J., Gerbig, C., Filges, A., Newberger, T., Sweeney, C., and Tans, P.: Accurate measurements of carbon monoxide in humid air using the cavity ring-down spectroscopy (CRDS) technique, Atmos. Meas. Tech., 6, 1031-1040, 2013.

Chen, P., Kang, S., Li, C., Rupakheti, M., Yan, F., Li, Q., Ji, Z., Zhang, Q., Luo, W., and Sillanpää, M.: Characteristics and sources of polycyclic aromatic hydrocarbons in atmospheric aerosols in the Kathmandu Valley, Nepal, Sci. Total Environ., 538, 86-92, 2015.

Chen, Y. H., and Prinn, R. G.: Estimation of atmospheric methane emissions between 1996 and 2001 using a three-dimensional global chemical transport model, J. Geophys. Res. Atmos., 111, 2006.

Conrad, R.: Soil microorganisms as controllers of atmospheric trace gases (H_2, CO, CH_4, OCS, N_2O, and NO), Microbiol. Rev., 60, 609-640, 1996.

Crosson, E.: A cavity ring-down analyzer for measuring atmospheric levels of methane, carbon dioxide, and water vapor, Appl. Phys. B: Lasers and Optics, 92, 403-408, 2008.

Department of Transport Management (DoTM).: Annual report of Ministry of Labor and Transport Management, Nepal Government, 2015.

Dlugokencky, E.J., A.M. Crotwell, P.M. Lang, J.W. Mund, Atmospheric Methane Dry Air Mole Fractions from quasi-continuous measurements at Mauna Loa, Hawaii, 1986-2016, Version: 2017-01-20, path: ftp://aftp.cmdl.noaa.gov/data/trace_gases/ch4/in-situ/surface/, 2017.

Dlugokencky, E.J., Lang, P.M., Crotwell, A. M., Mund, J. W., Crotwell, M. J., and Thoning, K. W.: Atmospheric Methane Dry Air Mole Fractions from the NOAA ESRL Carbon Cycle Cooperative Global Air Sampling Network, 1983-2015, Version: 2016-07-07, Path: ftp://aftp.cmdl.noaa.gov/data/trace_gases/ch4/flask/surface/, 2016.

Dlugokencky, E.J., Lang, P.M., Mund, J.W., Crotwell, A. M., Crotwell, M. J., and Thoning, K. W.: Atmospheric Carbon Dioxide Dry Air Mole Fractions from the NOAA ESRL Carbon Cycle Cooperative Global Air Sampling Network, 1968-2015, Version: 2016-08-30, Path: ftp://aftp.cmdl.noaa.gov/data/trace_gases/co2/flask/surface/, 2016a.

Fowler, A., and Hennessy, K.: Potential impacts of global warming on the frequency and magnitude of heavy precipitation, Nat. Hazards, 11, 283-303, 1995.

852 Fragkias, M., Lobo, J., Strumsky, D., and Seto, K. C.: Does size matter? Scaling of CO2
853 emissions and US urban areas, PLoS One, 8, e64727, 2013.
854
855 Ganesan, A., Chatterjee, A., Prinn, R., Harth, C., Salameh, P., Manning, A., Hall, B., Mühle, J.,
856 Meredith, L., and Weiss, R.: The variability of methane, nitrous oxide and sulfur hexafluoride in
857 Northeast India, Atmos. Chem. Phys., 13, 10633-10644, 2013.
858
859 Goroshi, S. K., Singh, R., Panigrahy, S., and Parihar, J.: Analysis of seasonal variability of
860 vegetation and methane concentration over India using SPOT-VEGETATION and ENVISAT-
861 SCIAMACHY data, J. Indian Soc. Remote, 39, 315-321, 2011.
862
863 International Centre for Integrated Mountain Development (ICIMOD).: Himalayas – Water for
864 1.3 Billion People. ICIMOD, Lalitpur, 2009.

865 Intergovernmental Panel for Climate Change (IPCC).: Climate Change 2013: The Physical
866 Science Basis. Contribution of Working Group I to the Fifth Assessment Report of the
867 Intergovernmental Panel on Climate Change, Cambridge University Press, Cambridge, United
868 Kingdom and New York, NY, USA, 2013.
869
870 Kim, B. M., Park, J.-S., Kim, S.-W., Kim, H., Jeon, H., Cho, C., Kim, J.-H., Hong, S.,
871 Rupakheti, M., and Panday, A. K.: Source apportionment of PM 10 mass and particulate carbon
872 in the Kathmandu Valley, Nepal, Atmos. Environ., 123, 190-199, 2015.
873
874 Kitada, T., and Regmi, R. P.: Dynamics of air pollution transport in late wintertime over
875 Kathmandu Valley, Nepal: As revealed with numerical simulation, J. Appl. Meteorol., 42, 1770-
876 1798, 2003.
877
878 Kumar, M. K., and Nagendra, S. S.: Characteristics of ground level CO_2 concentrations over
879 contrasting land uses in a tropical urban environment, Atmos. Environ., 115, 286-294, 2015.
880

881 Marinoni, A., Cristofanelli, P., Laj, P., Duchi, R., Putero, D., Calzolari, F., Landi, T.,
882 Vuillermoz, E., Maione, M., and Bonasoni, P.: High black carbon and ozone concentrations
883 during pollution transport in the Himalayas: Five years of continuous observations at NCO-P
884 global GAW station, J. Environ. Sci., 25, 1618-1625, 2013.
885
886 Ministry of Environment (MoE).: Status of climate change in Nepal, Kathmandu Nepal.
887 Kathmandu, Ministry of Environment, 2011.
888 Ministry of Environment and Forest (MoEF).: Indian Network for Climate Change Assessment:
889 India: Greenhouse Gas Emissions 2007, Tech. rep., 2007.
890 Mues, A., Rupakheti, M., Münkel, C., Lauer, A., Bozem, H., Hoor, P., Butler, T., and Lawrence,
891 M.: Investigation of the mixing layer height derived from ceilometer measurements in the
892 Kathmandu Valley and implications for local air quality. Atmos. Chem. Phys., doi:10.5194/acp-
893 2016-1002, in press, 2017.
894
895 Nepal Electricity Authority (NEA).: A year in review - fiscal year - 2013/2014
896 (http://www.nea.org.np/images/supportive_docs/Annual%20Report-2014.pdf), 2014.
897 NOAA ESRL Global Monitoring Division. updated annually.: Atmospheric Carbon Dioxide Dry
898 Air Mole Fractions from quasi-continuous measurements at Mauna Loa, Hawaii. Compiled by
899 K.W. Thoning, D.R. Kitzis, and A. Crotwell. National Oceanic and Atmospheric Administration
900 (NOAA), Earth System Research Laboratory (ESRL), Global Monitoring Division (GMD):
901 Boulder, Colorado, USA. Version 2016-8 at http://dx.doi.org/10.7289/V54X55RG, 2015.
902
903 Panday, A. K., and Prinn, R. G.: Diurnal cycle of air pollution in the Kathmandu Valley, Nepal:
904 Observations, J. Geophys. Res. Atmos., 114, 2009.
905
906 Panday, A. K., Prinn, R. G., and Schär, C.: Diurnal cycle of air pollution in the Kathmandu
907 Valley, Nepal: 2. Modeling results, Journal of Geophysical Research: Atmospheres, 114, 2009.

908 Patra, P., Niwa, Y., Schuck, T., Brenninkmeijer, C., Machida, T., Matsueda, H., and Sawa, Y.:
909 Carbon balance of South Asia constrained by passenger aircraft CO 2 measurements, Atmos.
910 Chem. Phys., 11, 4163-4175, 2011.
911
912 Pandey, A., Sadavarte, P., Rao, A. B., Venkataraman C.: Trends in multipollutant emissions
913 from a technology-linked inventory for India: II. Residential, agricultural and informal industry
914 sectors, Atmos. Environ., 99, 341-352, doi: 10.1016/j.atmosenv.2014.09.080, 2014.
915 Patra, P., Canadell, J., Houghton, R., Piao, S., Oh, N.-H., Ciais, P., Manjunath, K., Chhabra, A.,
916 Wang, T., and Bhattacharya, T.: The carbon budget of South Asia, 2013.
917
918 Patra, P., Niwa, Y., Schuck, T., Brenninkmeijer, C., Machida, T., Matsueda, H., and Sawa, Y.:
919 Carbon balance of South Asia constrained by passenger aircraft CO2 measurements, Atmos.
920 Chem. Phys., 11, 4163-4175, 2011.
921
922 Picarro.: Picarro G2401 CO2, CH4, CO, Water vapor CRDS analyzer
923 (http://hpst.cz/sites/default/files/attachments/datasheet-g2401-crds-analyzer-co2-co-ch4-h2o-air-
924 oct15-1.pdf), 2015.
925
926 Prasad, P., Rastogi, S., and Singh, R.: Study of satellite retrieved CO2 and CH4 concentration
927 over India, Adv. Space Res., 54, 1933-1940, 2014.
928
929 Pudasainee, D., Sapkota, B., Shrestha, M. L., Kaga, A., Kondo, A., and Inoue, Y.: Ground level
930 ozone concentrations and its association with NOx and meteorological parameters in Kathmandu
931 valley, Nepal, Atmos. Environ., 40, 8081-8087, 2006.
932
933 Putero, D., Landi, T., Cristofanelli, P., Marinoni, A., Laj, P., Duchi, R., Calzolari, F., Verza, G.,
934 and Bonasoni, P.: Influence of open vegetation fires on black carbon and ozone variability in the
935 southern Himalayas (NCO-P, 5079 m asl), Environ. Pollut., 184, 597-604, 2014.
936

Putero, D., Cristofanelli, P., Marinoni, A., Adhikary, B., Duchi, R., Shrestha, S., Verza, G., Landi, T., Calzolari, F., and Busetto, M.: Seasonal variation of ozone and black carbon observed at Paknajol, an urban site in the Kathmandu Valley, Nepal, Atmos. Chem. Phys., 15, 13957-13971, 2015.

Regmi, R. P., Kitada, T., and Kurata, G.: Numerical simulation of late wintertime local flows in Kathmandu valley, Nepal: Implication for air pollution transport, J. Appl. Meteorol., 42, 389-403, 2003.

Rodda, S.R., Thumaty, K. C., Jha, C. S. and Dadhwal, V. K.: Seasonal Variations of Carbon Dioxide, Water Vapor and Energy Fluxes in Tropical Indian Mangroves. Forests, 7, 35; doi:10.3390/f7020035, 2016.

Rupakheti, M., Panday, A. K., Lawrence, M. G., Kim, S. W., Sinha, V., Kang, S. C., Naja, M., Park, J. S., Hoor, P., Holben, B., Sharma, R. K., Mues, A., Mahata, K. S., Bhardwaj, P., Sarkar, C., Rupakheti, D., Regmi, R. P., and Gustafsson, Ö.: Air pollution in the Himalayan foothills: overview of the SusKat-ABC international air pollution measurement campaign in Nepal, Atmos. Chem. Phys., in preparation, 2017.

Sahu, L. K., and Lal, S.: Distributions of C 2–C 5 NMHCs and related trace gases at a tropical urban site in India. Atmos. Environ., 40(5), 880-891, 2006.

Sarangi, T., Naja, M., S.Lal, Venkataramani, S., Bhardwaj, P., Ojha, N., Kumar, R., Chandola, H. C.: First observations of light non-methane hydrocarbons (C2–C5) over a high altitude site in the central Himalayas, Atmos. Environ., 125, 450–460, 2016.

Sarangi T., Naja, M., Ojha, N., Kumar, R., Lal, S., Venkataramani, S., Kumar, A., Sagar, R., and Chandola, H. C.: First simultaneous measurements of ozone, CO and NOy at a high altitude regional representative site in the central Himalayas, J. Geophys. Res., 119, doi:10.1002/2013JD020631, 2014.

Sarkar, C., Sinha, V., Kumar, V., Rupakheti, M., Panday, A., Mahata, K. S., Rupakheti, D., Kathayat, B., and Lawrence, M. G.: Overview of VOC emissions and chemistry from PTR-TOF-MS measurements during the SusKat-ABC campaign: high acetaldehyde, isoprene and isocyanic acid in wintertime air of the Kathmandu Valley, Atmos. Chem. Phys., 16, 3979-4003, 2016.

Schneising, O., Buchwitz, M., Burrows, J., Bovensmann, H., Bergamaschi, P., and Peters, W.: Three years of greenhouse gas column-averaged dry air mole fractions retrieved from satellite–Part 2: Methane, Atmos. Chem. Phys., 9, 443-465, 2009.

Sharma, R., Bhattarai, B., Sapkota, B., Gewali, M., and Kjeldstad, B.: Black carbon aerosols variation in Kathmandu valley, Nepal, Atmos. Eenviron., 63, 282-288, 2012.

Shrestha, R. M., and Rajbhandari, S.: Energy and environmental implications of carbon emission reduction targets: Case of Kathmandu Valley, Nepal, Energ.y Policy, 38, 4818-4827, 2010.

Shrestha, S. R., Oanh, N. T. K., Xu, Q., Rupakheti, M., and Lawrence, M. G.: Analysis of the vehicle fleet in the Kathmandu Valley for estimation of environment and climate co-benefits of technology intrusions, Atmos. Environ., 81, 579-590, 2013.

Sinha, V., Kumar, V., and Sarkar, C.: Chemical composition of pre-monsoon air in the Indo-Gangetic Plain measured using a new air quality facility and PTR-MS: high surface ozone and strong influence of biomass burning, Atmos. Chem. Phys., 14, 5921-5941, 10.5194/acp-14-5921-2014, 2014.

Smith, K. R., Uma, R., Kishore, V., Zhang, J., Joshi, V., and Khalil, M.: Greenhouse implications of household stoves: an analysis for India, Ann. Rev. Energ. Environ., 25, 741-763, 2000.

Sreenivas, G., Mahesh, P., Subin, J., Kanchana, A. L., Rao, P. V. N., and Dadhwal, V. K.: Influence of Meteorology and interrelationship with greenhouse gases (CO_2 and CH_4) at a suburban site of India, Atmos. Chem. Phys., 16, 3953-3967, 2016.

Stockwell, C. E., Christian, T. J., Goetz, J. D., Jayarathne, T., Bhave, P. V., Praveen, P. S., Adhikari, S., Maharjan, R., DeCarlo, P. F., and Stone, E. A.: Nepal ambient monitoring and source testing experiment (NAMaSTE): emissions of trace gases and light-absorbing carbon from wood and dung cooking fires, garbage and crop residue burning, brick kilns, and other sources, Atmos.pheric Chem. Phys., 16, 11043-11081, 2016.

Westerdahl, D., Wang, X., Pan, X., and Zhang, K. M.: Characterization of on-road vehicle emission factors and microenvironmental air quality in Beijing, China, Atmos. Environ., 43, 697-705, 2009.

Weyant, C., Athalye, V., Ragavan, S., Rajarathnam, U., Lalchandani, D., Maithel, S., Baum, E., and Bond, T. C.: Emissions from South Asian brick production, Environ. Sci. Tech., 48, 6477-6483, 2014.

World Bank.: Managing Nepal's Urban Transition (http://www.worldbank.org/en/news/feature/2013/04/01/managing-nepals-urban-transition), 2013.

World Bank.: Diesel power generation: inventories, black carbon emissions in Kathmandu Valley, Nepal. Washington. The World Bank: 1818H Street NW, Washington, DC 20433, USA

WMO.: The state of greenhouse gases in the atmosphere based on global observations through 2015(http://reliefweb.int/sites/reliefweb.int/files/resources/GHG_Bulletin_12_EN_web_JN161640.pdf), 2016.

Table 1. Instruments and sampling at Bode (semi-urban site) and Chanban (rural site)

Site	Instrument	Species	Sampling interval	Measurement period	Inlet/sensor height above ground (m)
Bode	i. Cavity ring down spectrometer (Picarro G2401, USA)	CO_2, CH_4, CO, water vapor	5 sec	06 Mar 2013 - 05 Mar 2014 14 Jul 2015 - 07 Aug 2015	20
	ii. CO monitor (Horriba AP370, USA)	CO	5 min	06 Mar 2013 – 07 June 2013	20
	iii. Ceilometer (Vaisala CL31, Finland		15-52 min	06 Mar 2013 – 05 Mar 2014	15
	iv. AWS (Campbell Scientific, USA)		1 min		23
	a. CS215	RH, T		06 Mar 2013 – 24 Apr 2013	
	b. CS300 Pyranometer	SR		06 Mar 2013 - 05 Mar 2014 14 Jul 2015 - 07 Aug 2015	
	c. RM Young 05103-5	WD, WS		06 Mar 2013 - 05 Mar 2014 14 July 2015 - 07 Aug 2015	
	v. Airport AWS (Environdata, Australia)				
	a. TA10	T		18 Jun 2013 – 13 Jan 2013	
	b. RG series	RF		06 Mar 2013 – 15 Dec 2013	
Chanban	i. Cavity ring down spectrometer (Picarro G2401, USA)	CO_2, CH_4, CO, water vapor	5 sec	15 July 2015 - 03 Oct 2015	3
	ii AWS (Davis Vantage Pro2, USA)	RH, T, SR, WD, WS, RF, P	10 min	14 July 2015 - 07 Aug 2015	2

AWS: Automatic weather station, RH: ambient relative humidity, T: ambient temperature, SR: global solar radiation, WS: wind speed, WD: wind direction, RF: rainfall, P: ambient pressure

Table 2. Summary of monthly average CH_4 and CO_2 mixing ratios observed at Bode, a semi-urban site in the Kathmandu Valley during March 2013 to Feb 2014 [mean, standard deviation (SD), median, minimum (Min.), maximum (Max.) and number of data points of hourly average values]

	CH_4 (ppm)					CO_2 (ppm)					Data points
Month	Mean	SD	Median	Min.	Max.	Mean	SD	Median	Min.	Max.	
Mar	2.207	0.245	2.152	1.851	3.094	426.6	26.4	418.3	378.8	510.8	596
Apr	2.183	0.252	2.094	1.848	3.121	430.3	27.4	421.0	397.0	536.9	713
May	2.093	0.174	2.040	1.863	2.788	421.7	22.1	413.4	395.9	511.2	725
Jun	2.061	0.142	2.017	1.869	2.675	417.9	21.3	410.4	390.5	495.7	711
Jul	2.129	0.168	2.074	1.893	2.770	410.3	18.2	406.3	381.0	471.0	500
Aug	2.274	0.260	2.181	1.953	3.219	409.9	22.8	405.3	376.1	493.1	737
Sep	2.301	0.261	2.242	1.941	3.331	414.9	30.2	404.0	375.9	506.2	710
Oct	2.210	0.195	2.156	1.927	2.762	417.0	25.1	411.8	381.9	486.7	743
Nov	2.207	0.203	2.178	1.879	2.705	417.2	20.7	415.7	385.7	478.9	717
Dec	2.206	0.184	2.193	1.891	2.788	417.7	17.3	418.0	386.7	467.6	744
Jan	2.233	0.219	2.198	1.889	2.744	424.8	20.9	422.3	392.7	494.5	696
Feb	2.199	0.223	2.152	1.877	2.895	423.2	22.0	417.9	392.2	484.6	658
Annual	2.1923	0.066	2.140	1.848	3.331	419.3	6.0	413.7	375.9	536.9	

Table 3. Summary of CH_4 and CO_2 mixing ratios at Bode across four seasons during March 2013 to Feb 2014 [seasonal mean, one standard deviation (SD), median, minimum (Min.) and maximum (Max.)]

	CH_4 (ppm)					CO_2 (ppm)				
Season	Mean	SD	Median	Min.	Max.	Mean	SD	Median	Min.	Max.
Pre-Monsoon	2.157	0.230	2.082	1.848	3.121	426.2	25.5	417.0	378.8	536.9
Monsoon	2.199	0.241	2.126	1.869	3.331	413.5	24.2	407.1	375.9	506.2
Post-Monsoon	2.210	0.200	2.167	1.879	2.762	417.3	23.1	414.1	381.9	486.7
Winter	2.214	0.209	2.177	1.877	2.895	421.9	20.3	419.3	386.7	494.5

Table 4. Comparison of monthly average CH_4 and CO_2 mixing ratios at a semi-urban and a rural site in Nepal (this study) with other urban and background sites in the region and elsewhere.

Site Setting	Bode, Nepal (Urban)				Chanban, Nepal (Rural)		Mauna Loa, USA (Background)[c]		Waliguan, China (Background)[d]	
Species	CO_2	CH_4	*CO_2	*CH_4	*CO_2	*CH_4	CO_2	CH_4	CO_2	CH_4
Unit	Ppm	ppm	Ppm	Ppm	Ppm	Ppm	Ppm	ppm	Ppm	ppm
Mar 2013	426.6	2.207					397.3	1.840	399.5	1.868
Apr	430.3	2.183					398.4	1.837	402.8	1.874
May	421.7	2.093					399.8	1.834	402.5	1.878
Jun	417.9	2.061					398.6	1.818	397.4	1.887
Jul	410.3	2.129					397.2	1.808	393.3	1.888
Aug	409.9	2.274	411.3	2.281	403.4	2.050	395.2	1.819	392.0	1.893
Sep	414.9	2.301	419.9	2.371	399.1	2.102	393.5	1.836	393.1	1.894
Oct	417.0	2.210					393.7	1.836	395.6	1.876
Nov	417.2	2.207					395.1	1.835	397.1	1.875
Dec	417.7	2.206					396.8	1.845	398.6	1.880
Jan 2014	424.8	2.234					397.8	1.842	398.8	1.865
Feb	423.2	2.199					397.9	1.834	401.1	1.878
Annual										
Bode	419.3	2.192								
Mauna Loa							396.8	1.832		
Waliguan									397.7	1.880
Shadnagar (2014)[a]	394.0									
Ahemadabad (2013-2015)[b]	413.0	1.920								

*The monthly values for CO_2 and CH_4 in 2015, [a]Sreenivas et al., 2016, [b]Chandra et al., 2016, [c]Dlugokencky et al., 2017; NOAA, 2015, [d] Dlugokencky et al., 2016; Dlugokencky et al., 2016a.

Table 5. Emission ratio of CO/CO_2 (ppb ppm^{-1}) derived from emission factors (mass of gas emitted from per kilogram of fuel burned, "except for the transport sector" which is derived from gram of gases emitted per kilometer distance travelled)

Sectors	Details	CO/CO_2	Reference
1. Residential/Commercial			
i. LPG		4.8	Smith et al. (2000)
ii. Kerosene		13.4	Smith et al. (2000)
iii. Biomass		52.9 - 98.5	*
iv. Diesel power generators	< 15 year old	5.8	The World Bank (2014)
	> 15 year old	4.5	
2. Transport			**
a. Diesel			
i. HCV diesel bus	> 6000cc, 1996-2000	4.9	
	post 2000 and 2005	5.4	
ii. HCV diesel truck	> 6000cc, post 2000	7.9	
b. Petrol			
i. 4 stroke motorcycle	< 100 cc, 1996-2000	68	
	100-200 cc, Post 2000	59.6	
ii. Passenger cars	< 1000 cc, 1996-2000	42.4	
iii. Passenger cars	< 1000 cc, Post 2000	10.3	
3. Brick industries			
i. BTK fixed kiln		17.2	Weyant et al. (2014)
ii. Clamp brick kiln		33.7	Stockwell et al. (2016)
iii. Zigzag brick kiln		3.9	Stockwell et al. (2016)
4. Open burning			
i. Mixed garbage		46.9	Stockwell et al. (2016)
ii. Crop-residue		51.6	Stockwell et al. (2016)

* Westerdahl et al. (2009)

** http://www.cpcb.nic.in/Emission_Factors_Vehicles.pdf

Table 6. Average (SD) of the ratio of dCO to dCO_2, their Geometric mean (GeoSD) over a period of 3 hours during (a) morning peak (b) evening peak and (c) seasonal (all hours) of the ambient mixing ratios of CO and CO_2 and their lower and upper bound (LB and UB).

Period	Season	Mean (SD)	Median	N	Geomean (GeoSD)	LB	UB
a. Morning hours (7:00-9:00)	Pre-monsoon	7.6 (3.1)	7.8	249	11.3 (1.5)	5.2	24.8
	Monsoon	2.2 (1.6)	1.9	324	9.9 (1.9)	2.7	36.3
	Post-monsoon	3.1 (1.4)	2.8	183	11.1 (1.5)	4.7	26.3
	Winter*	11.2 (4.4)	11	255	11.4 (1.5)	5.3	24.2
b. Evening hours (19:00-21:00)	Pre-monsoon	15.1 (9.0)	12.7	248	10.5 (1.7)	3.5	31.6
	Monsoon	8.0 (5.2)	6.3	323	10.2 (1.8)	3.1	33.5
	Post-monsoon	11.5 (5.6)	10.6	182	11.0 (1.6)	4.4	27.6
	Winter	21.6 (14.1)	18.2	254	10.2 (1.8)	3.1	33.6
c. Seasonal (all hours)	Pre-monsoon	12.2 (13.3)	8.8	1740	8.2 (2.4)	1.4	48.4
	Monsoon	7.5 (13.5)	2.9	2176	5.9 (3.3)	0.5	65.6
	Post-monsoon	8.3 (12.4)	4.4	1289	6.8 (3.0)	0.8	59.2
	Winter	15.1 (13.3)	12.5	1932	9.2 (2.1)	2.0	41.7

*The morning peak was one hour delayed in winter, thus the 8:00-10:00 period data was used in the analysis.

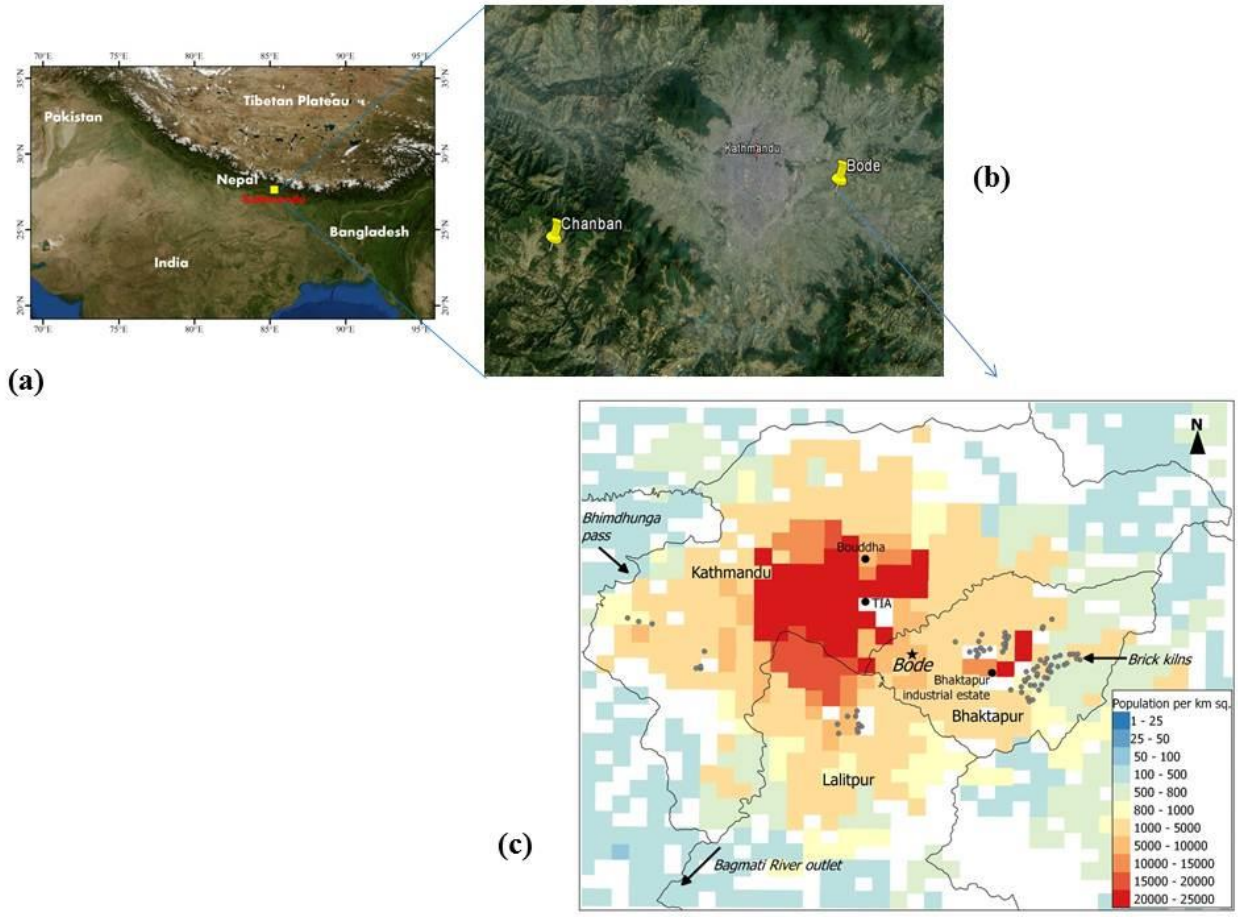

Figure 1. Location of measurement sites: (a) Kathmandu Valley (b) semi-urban measurement site at Bode in Kathmandu Valley, and a rural measurement site at Chanban in Makawanpur district Nepal, (c) general setting of Bode site. Colored grid and TIA represent population density and the Tribhuvan International Airport, respectively.

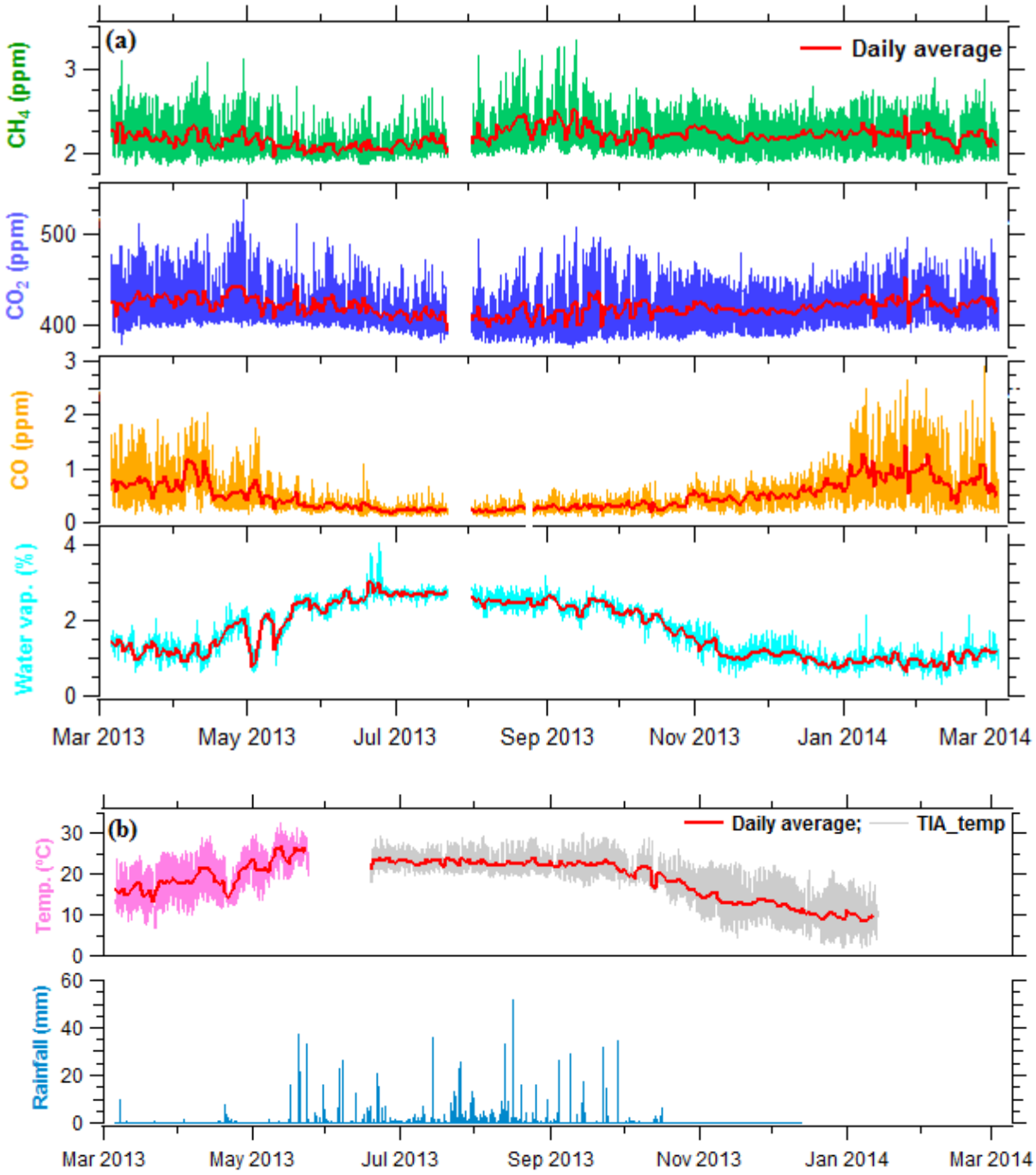

Figure 2. Time series of hourly average (a) mixing ratios of CH_4, CO_2, CO, and water vapor measured with a cavity ring down spectrometer (Picarro G2401) at Bode, and (b) temperature and rainfall monitored at the Tribhuvan International Airport (TIA), ~4 km to the west of Bode site in the Kathmandu Valley, Nepal. Temperature shown in pink color is observed at Bode site.

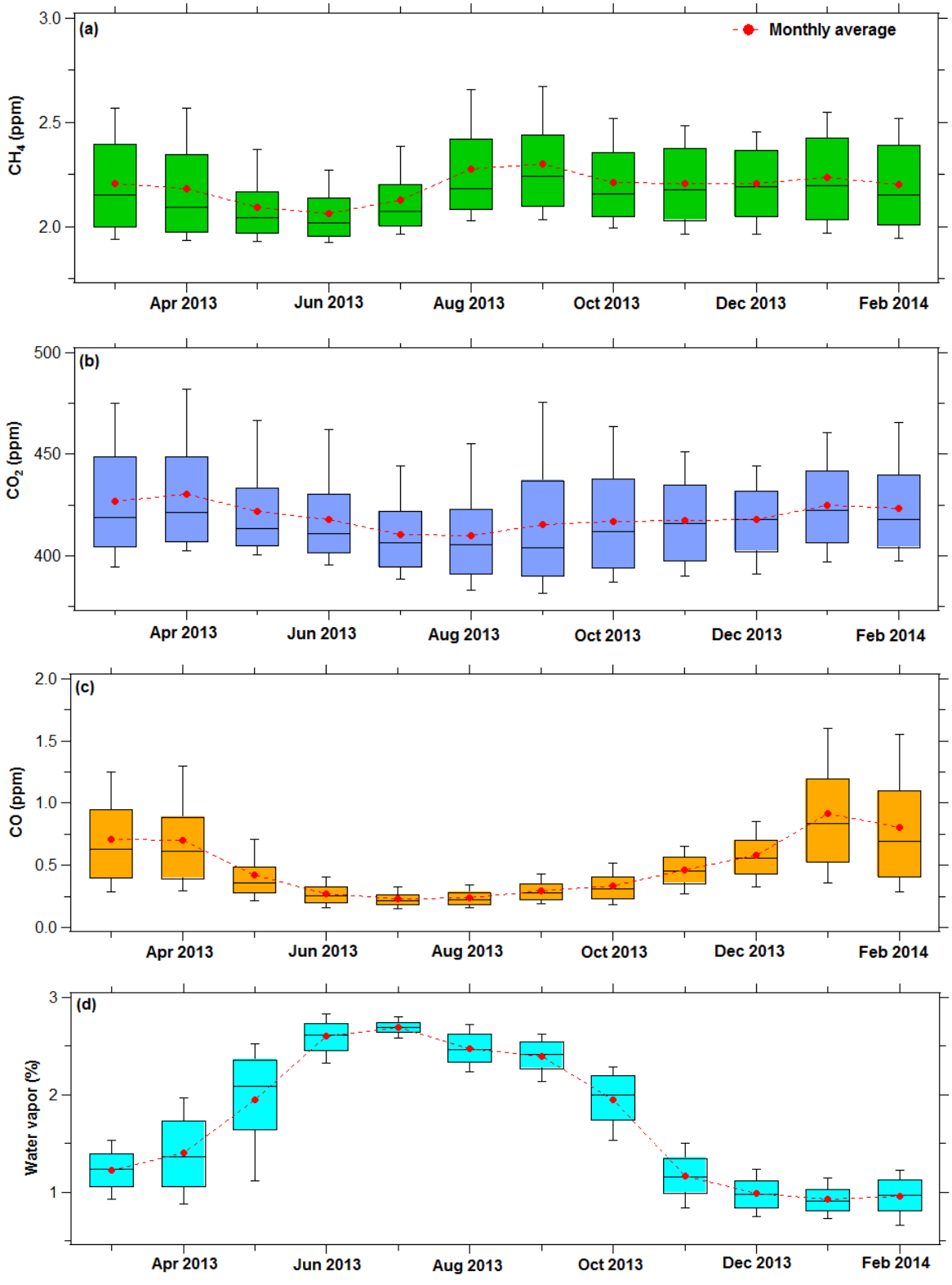
(a)
Monthly average
CH4 (ppm)
3.0
2.5
2.0
(b)
CO2 (ppm)
500
450
400
(c)
CO (ppm)
2.0
1.5
1.0
0.5
0.0
(d)
Water vapor (%)
3
2
1
Apr 2013
Jun 2013
Aug 2013
Oct 2013
Dec 2013
Feb 2014

Figure 3. Monthly variations of the mixing ratios of hourly (a) CH_4, (b) CO_2, (c) CO, and (d) water vapor observed at a semi-urban site (Bode) in the Kathmandu Valley over a period of a year. The lower end and upper end of the whisker represents 10^{th} and 90^{th} percentile, respectively; the lower end and upper end of each box represents 25^{th} and 75^{th} percentile, respectively, and black horizontal line in the middle of each box is the median for each month while red dot represents mean for each month.

(a)

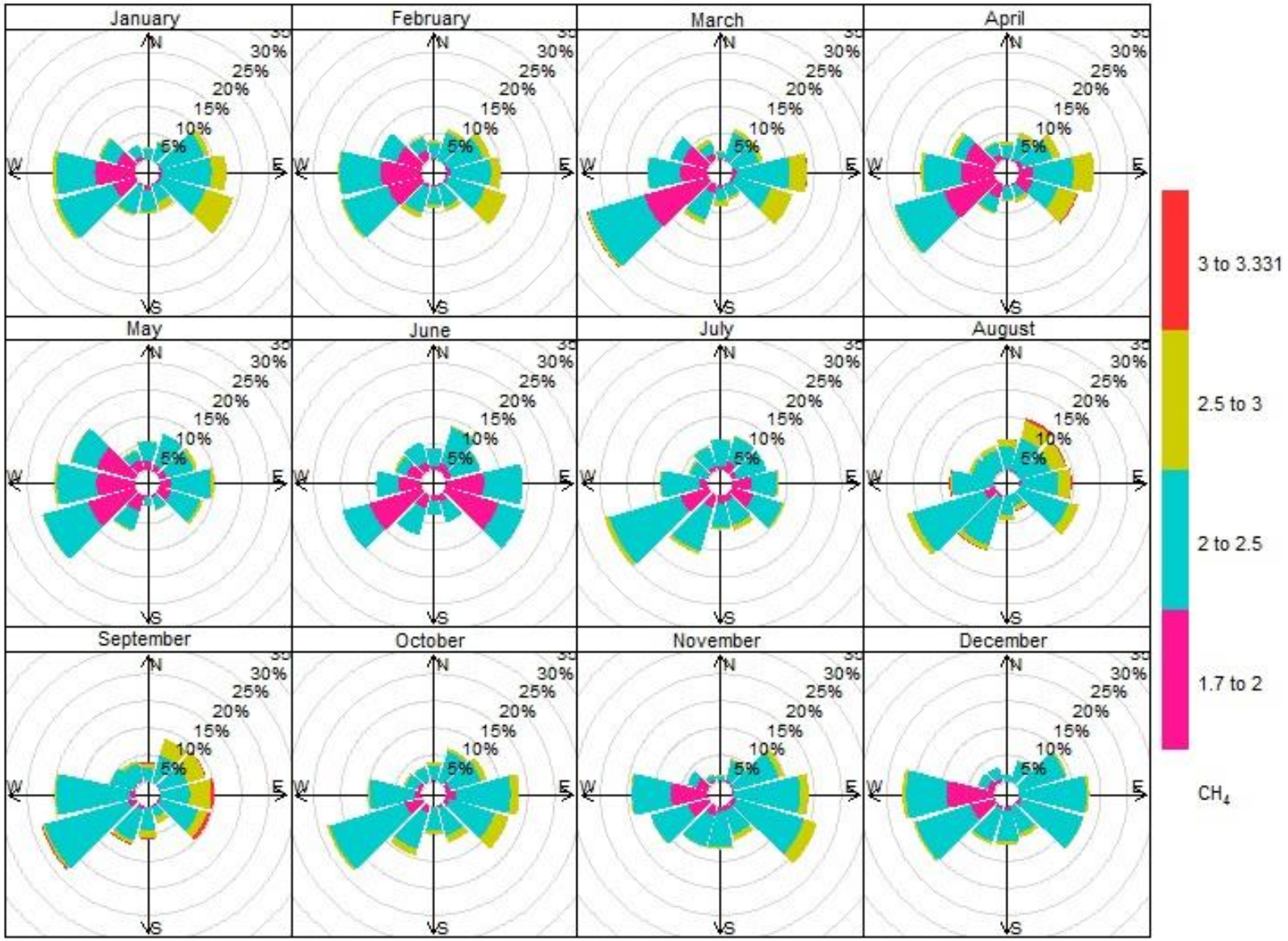
January
February
March
April
May
June
July
August
September
October
November
December
N
S
E
W
5%
10%
15%
20%
25%
30%
3 to 3.331
2.5 to 3
2 to 2.5
1.7 to 2
CH4

(b)

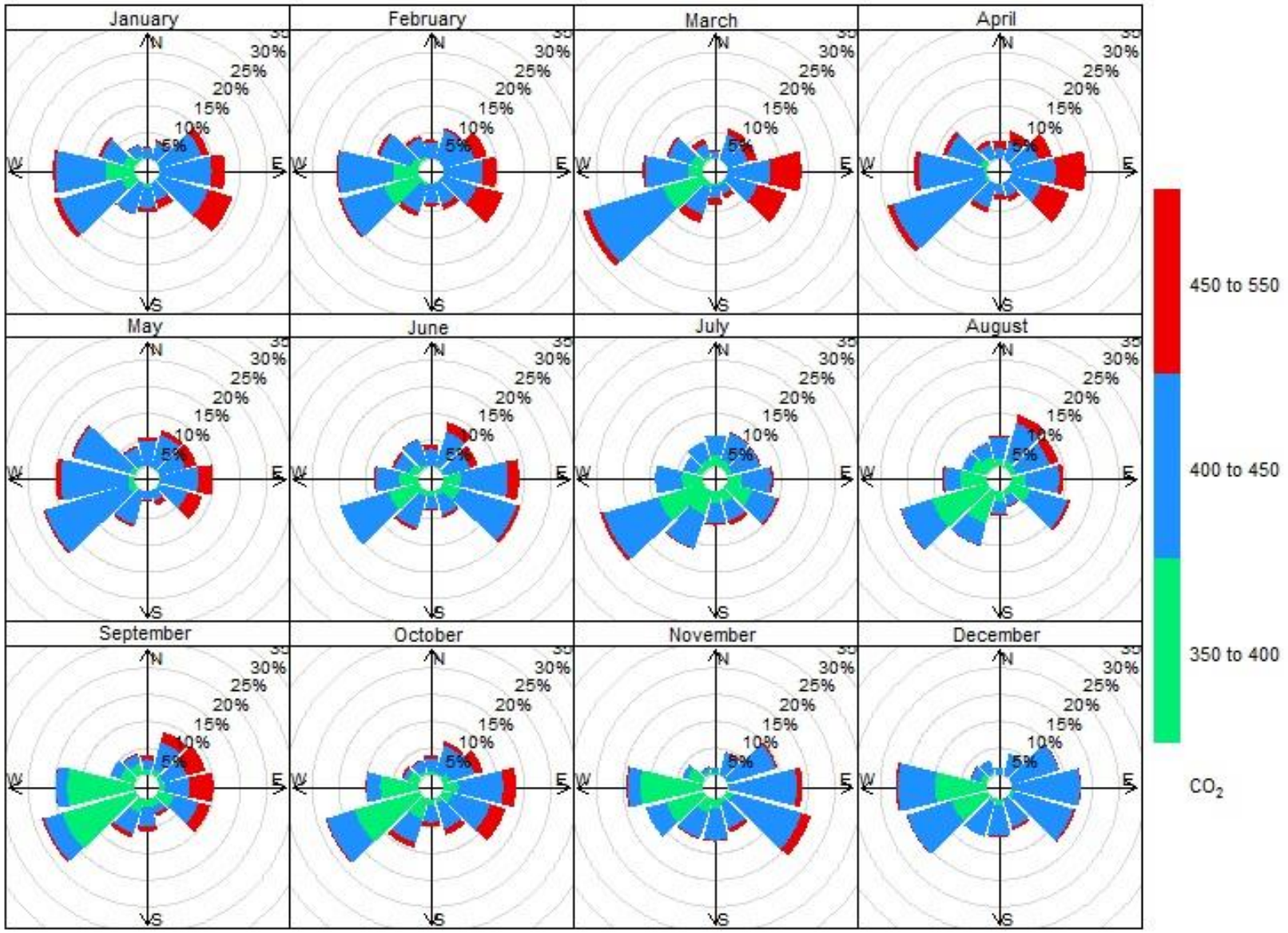
January
February
March
April
May
June
July
August
September
October
November
December
N
S
E
W
5%
10%
15%
20%
25%
30%
450 to 550
400 to 450
350 to 400
CO_2

(c)

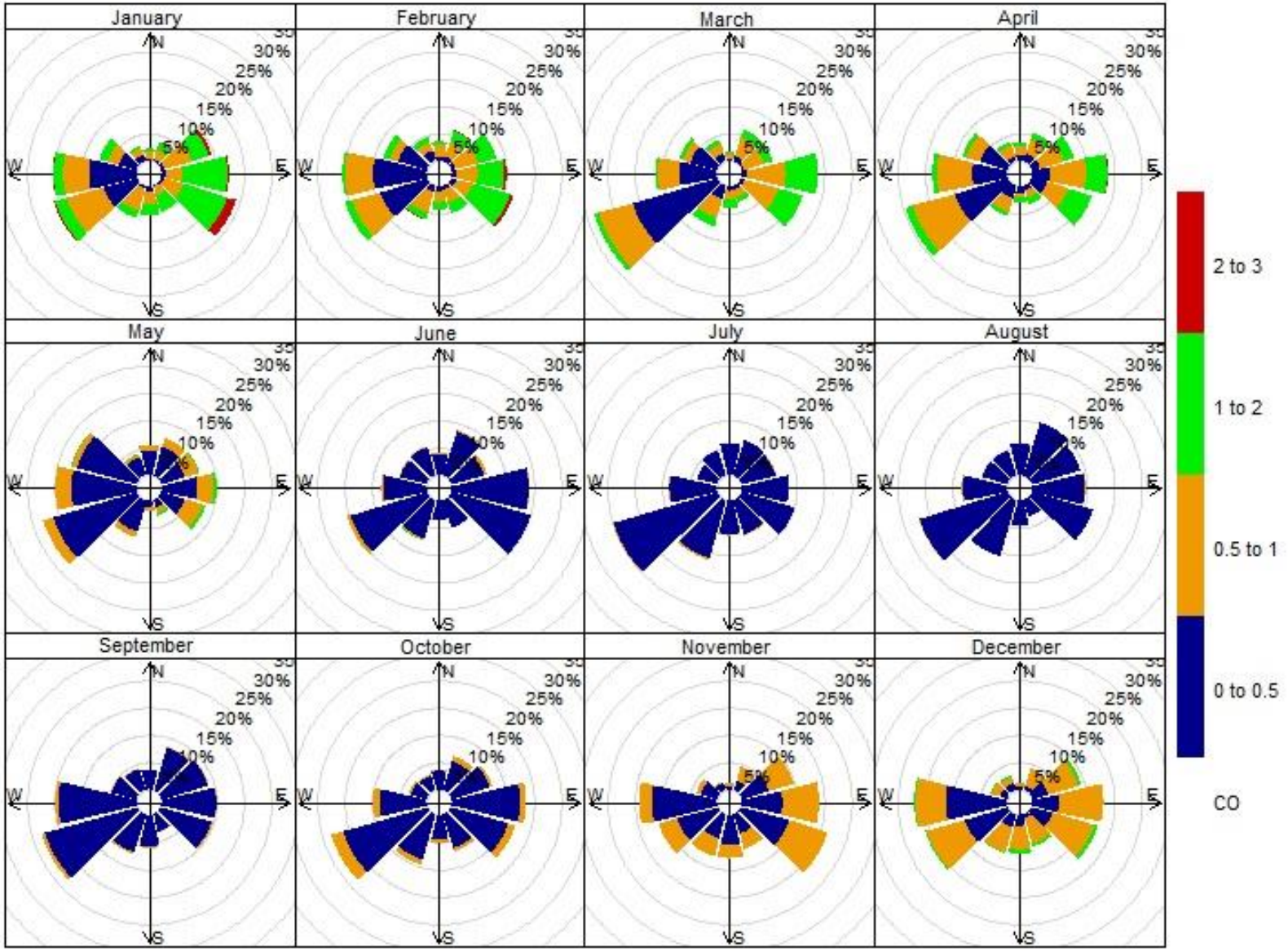
January
February
March
April
May
June
July
August
September
October
November
December
N
S
E
W
5%
10%
15%
20%
25%
30%
2 to 3
1 to 2
0.5 to 1
0 to 0.5
CO

Figure 4. Relation between mixing ratios and wind direction observed at Bode in the Kathmandu Valley (a) CH_4, (b) CO_2 and (c) CO from March 2013 to February 2014. The figure shows variations of CH_4, CO_2 and CO mixing ratios based on frequency counts of wind direction (in %) as represented by circle. The color represents the different mixing ratios of the gaseous species. The units of CH_4, CO_2 and CO are in ppm.

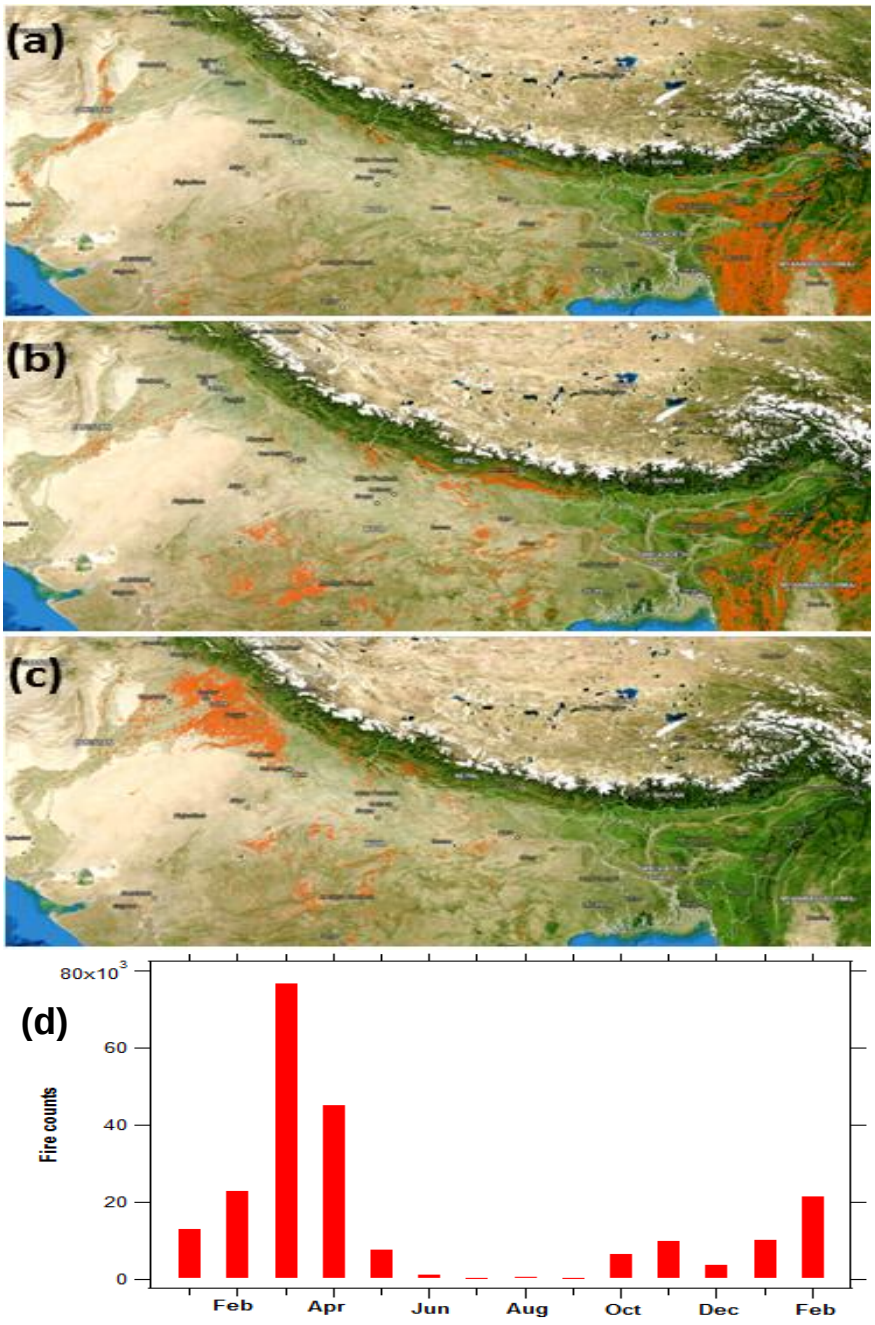

Figure 5. Satellite detected fire counts in (a) Mar, (b) Apr, (c) May 2013 in the broader region surrounding Nepal and (d) total number of fire counts detected by MODIS instrument onboard the Aqua satellite during Jan 2013-Feb 2014. Source: https://firms.modaps.eosdis.nasa.gov/firemap/

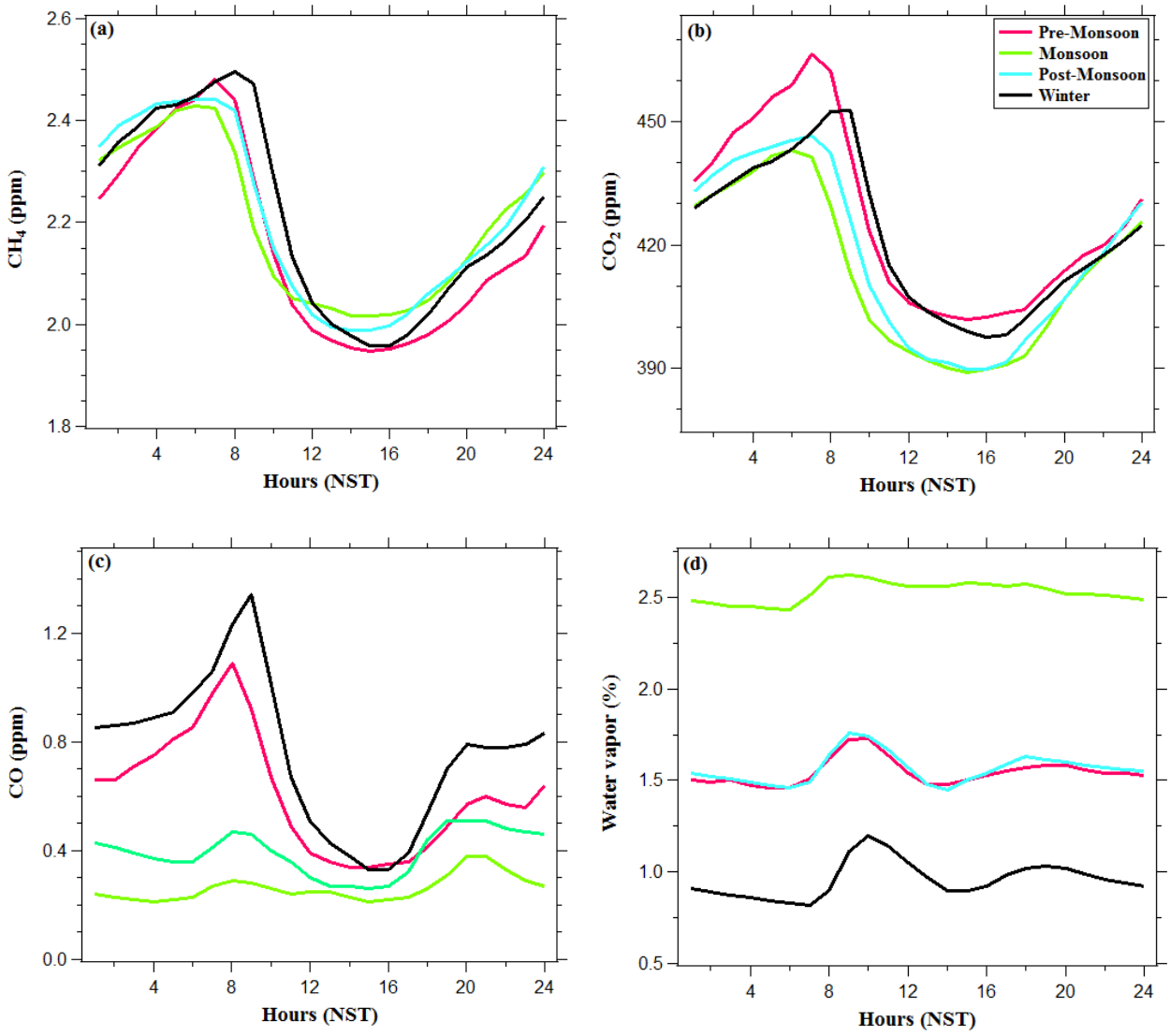

Figure 6. Diurnal variations of hourly mixing ratios in different seasons (a) CH_4, (b) CO_2, (c) CO, and (d) water vapor observed at Bode (semi-urban site) in the Kathmandu Valley during March 2013-February 2014. Seasons are defined as Pre-monsoon: Mar-May, Monsoon: Jun-Sep, Post-monsoon: Oct-Nov, Winter: Dec-Feb. The x axis is in Nepal Standard Time (NST).

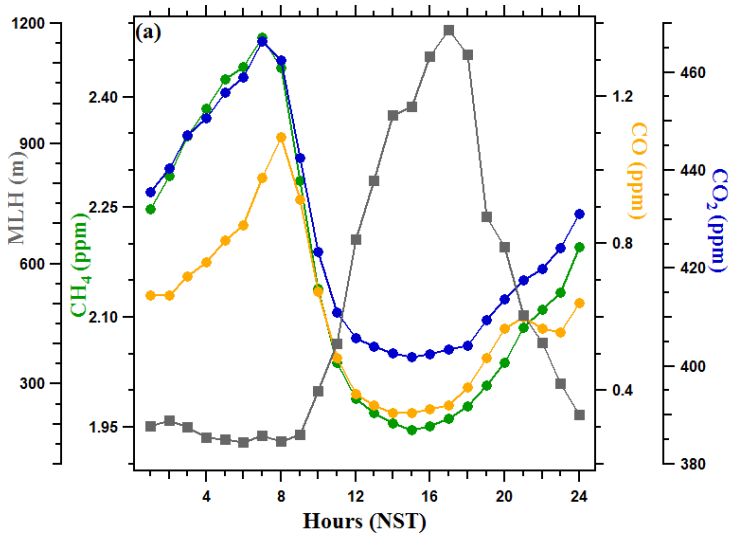
(a)
MLH (m)
CH4 (ppm)
CO (ppm)
CO2 (ppm)
Hours (NST)

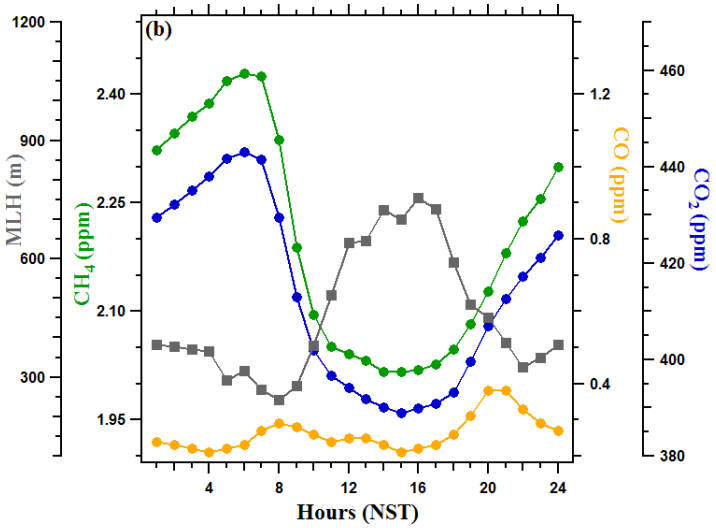
(b)
MLH (m)
CH4 (ppm)
CO (ppm)
CO2 (ppm)
Hours (NST)

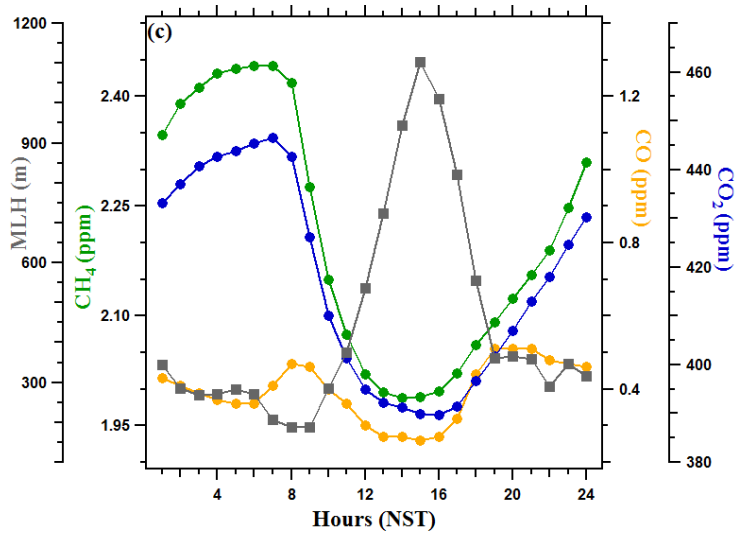
(c)
MLH (m)
CH4 (ppm)
CO (ppm)
CO2 (ppm)
Hours (NST)

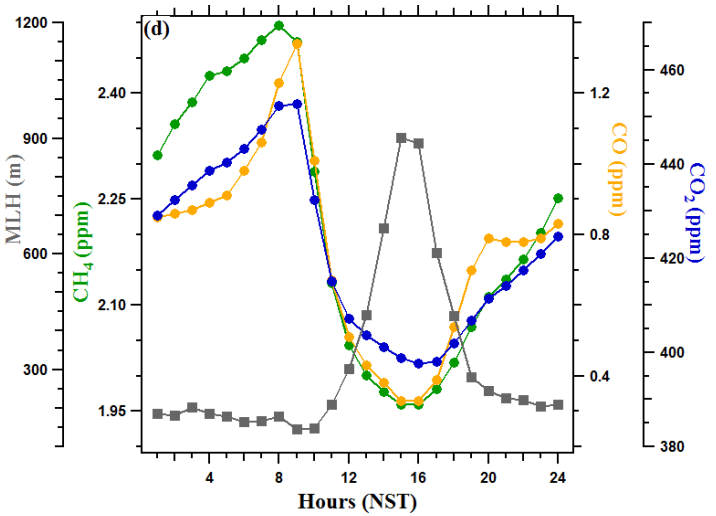
(d)
MLH (m)
CH4 (ppm)
CO (ppm)
CO2 (ppm)
Hours (NST)

Figure 7. Diurnal variations of hourly mixing ratios of CH_4, CO_2, CO, and mixing layer height (MLH) at Bode (a semi-urban site in the Kathmandu Valley) in different seasons (a) pre-monsoon (Mar-May), (b) monsoon (Jun-Sep), (c) post-monsoon (Oct-Nov) and (d) winter (Dec-Feb) during March 2013- Feb 2014.

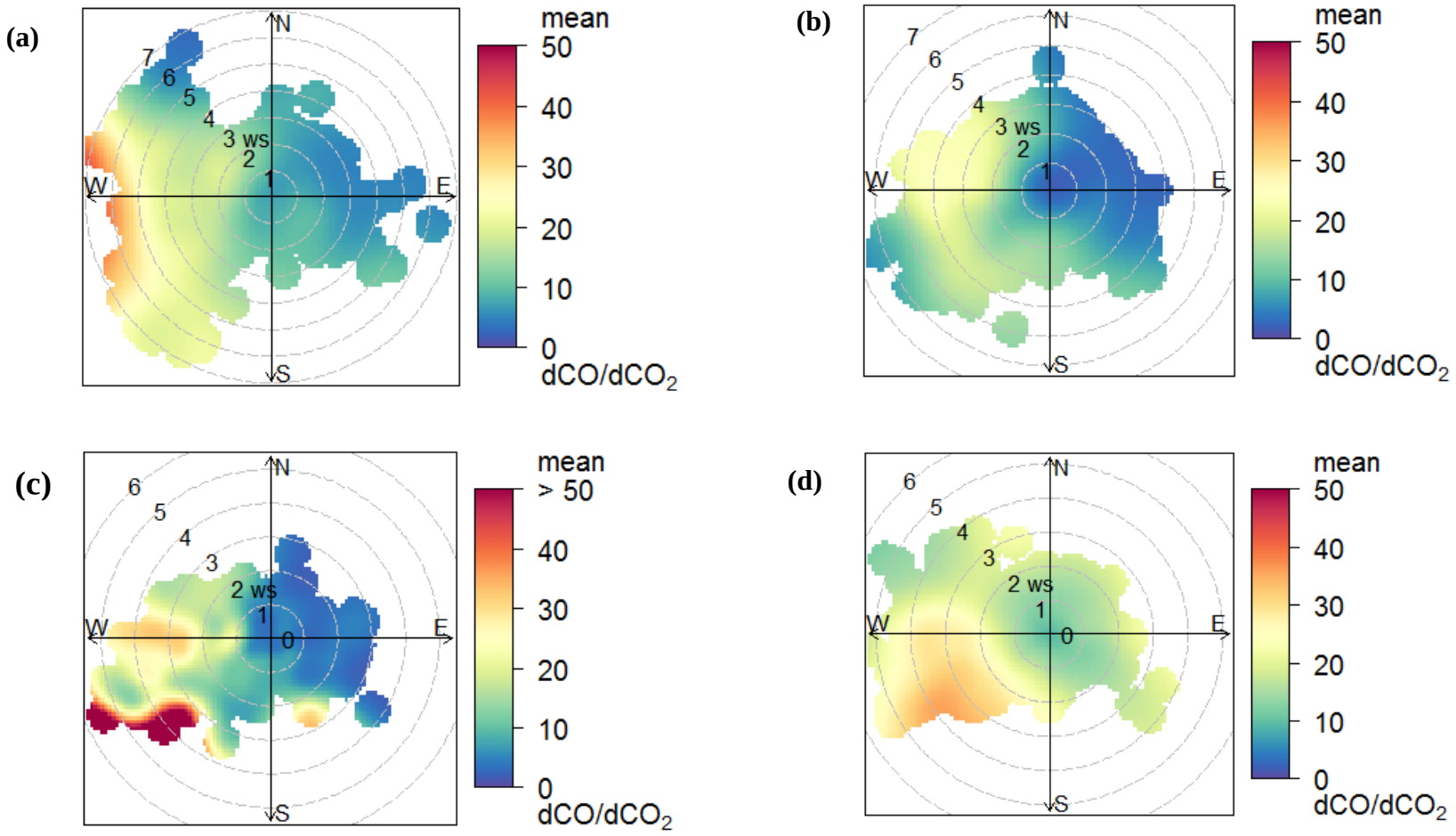

Figure 8. Seasonal polar plot of hourly dCO/dCO_2 ratio based upon wind direction and wind speed: (a) pre-monsoon, (b) monsoon, (c) post-monsoon and (d) winter seasons.

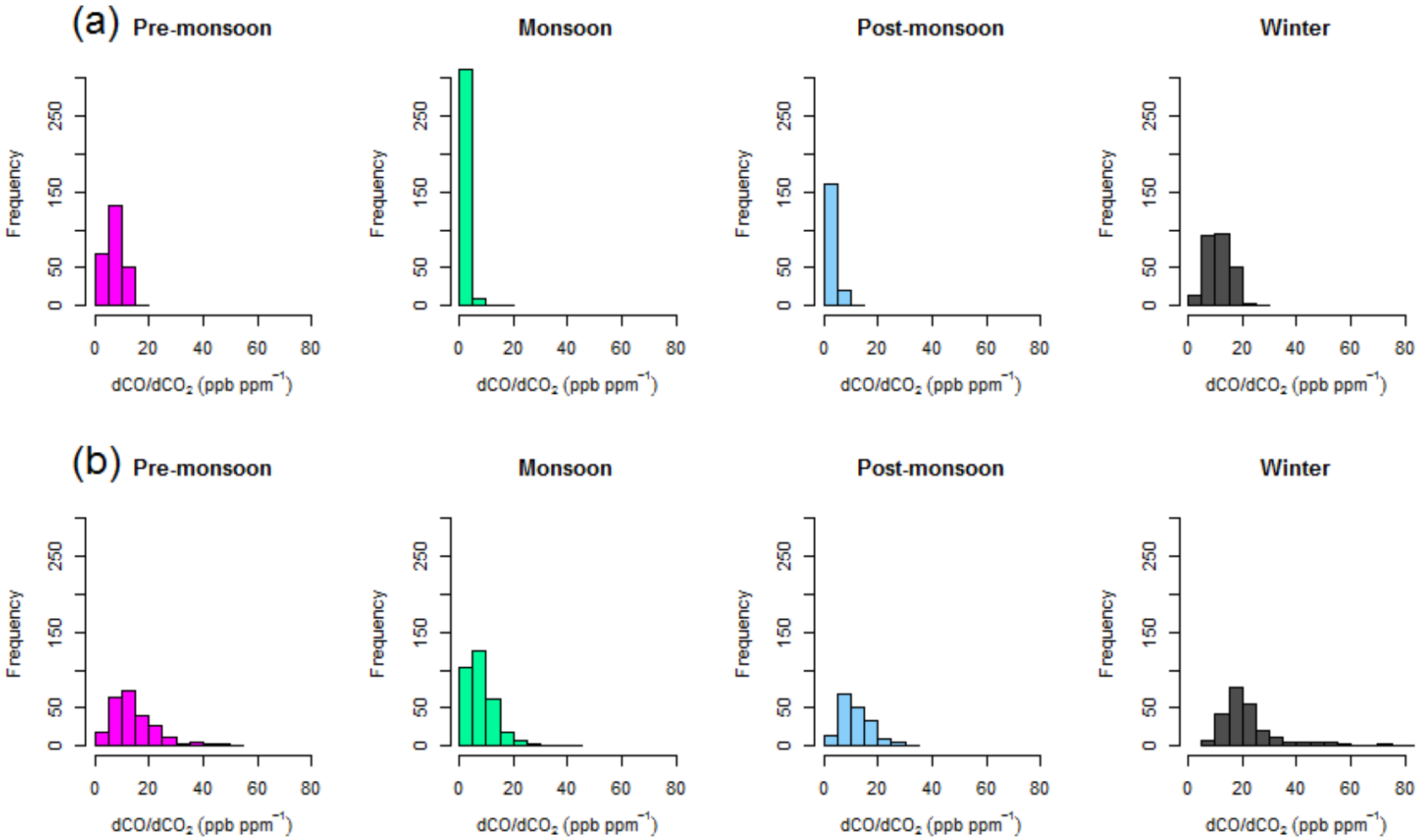

Figure 9. Seasonal frequency distribution of hourly dCO/dCO_2 ratio (a) morning hours (7:00-9:00) in all seasons except winter (8:00-10:00), (b) evening hours (19:00-21:00)

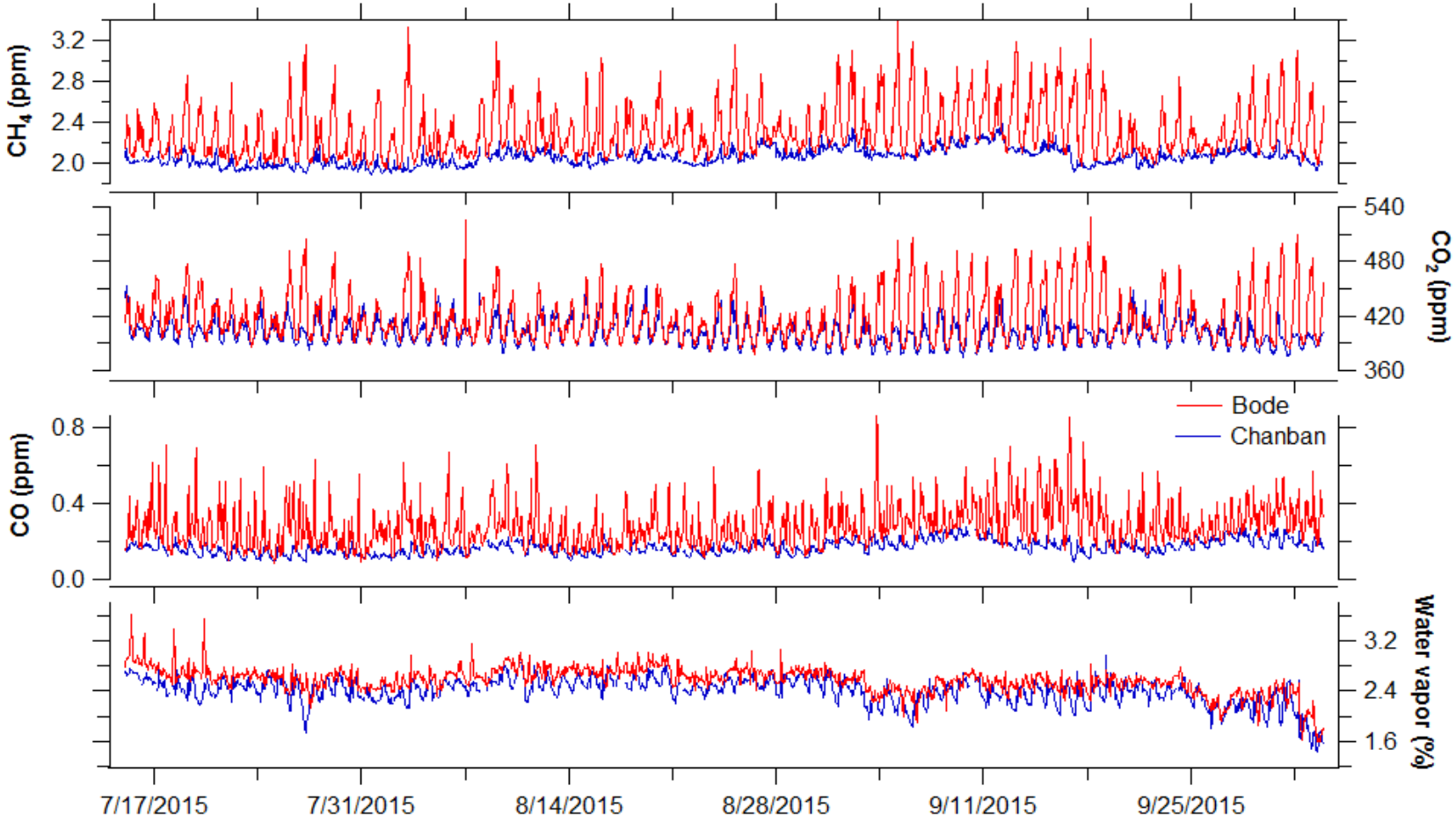

Figure 10. Comparison of hourly average mixing rations of CH_4, CO_2, CO, and water vapor observed at Bode (a semi-urban site) in the Kathmandu Valley and at Chanban (a rural/background site) in Makawanpur district, ~ 20 km from Kathmandu, on other side of a tall ridge.

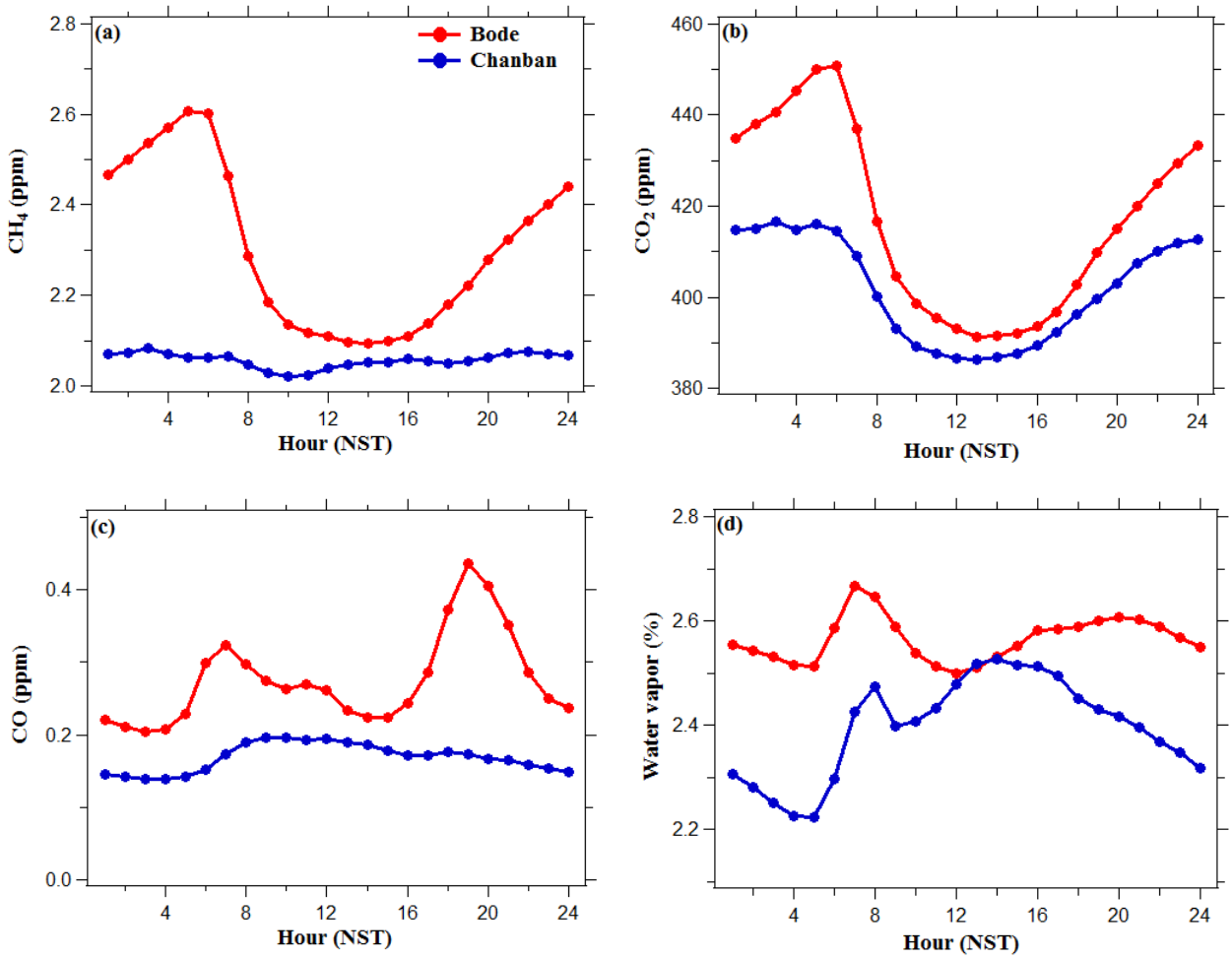

Figure 11. Diurnal variations of hourly average mixing ratios of (a) CH_4, (b) CO_2, (c) CO and (d) water vapor observed at Bode in the Kathmandu Valley and at Chanban in Makawanpur district during 15 July- 03 October 2015.